

1,3-Benzodioxole-Modified Noscapine Analogues: Synthesis, Antiproliferative Activity, and Tubulin-Bound Structure

Cassandra Yong,^[a] Shane M. Devine,^{+, [a]} Anne-Catherine Abel,^{+, [b]} Stefan D. Tomlins,^[a] Divya Muthiah,^[c] Xuexin Gao,^[c] Richard Callaghan,^[c] Michel O. Steinmetz,^[b, d] Andrea E. Prota,^{*, [b]} Ben Capuano,^{*, [a]} and Peter J. Scammells^{*, [a]}

Since the revelation of noscapine's weak anti-mitotic activity, extensive research has been conducted over the past two decades, with the goal of discovering noscapine derivatives with improved potency. To date, noscapine has been explored at the 1, 7, 6', and 9'-positions, though the 1,3-benzodioxole motif in the noscapine scaffold that remains unexplored. The present investigation describes the design, synthesis and pharmacological evaluation of noscapine analogues consisting of modifications to the 1,3-benzodioxole moiety. This includes expansion of the dioxolane ring and inclusion of metabolically robust deuterium and fluorine atoms. Favourable structural modifications were subsequently incorporated into multi-functionalised noscapine derivatives that also possessed modifications previously shown to promote anti-proliferative activity in the 1-, 6'- and 9'-positions. Our research efforts afforded the

deuterated noscapine derivative **14e** and the dioxino-containing analogue **20** as potent cytotoxic agents with EC₅₀ values of 1.50 and 0.73 μ M, respectively, against breast cancer (MCF-7) cells. Compound **20** also exhibited EC₅₀ values of < 2 μ M against melanoma, non-small cell lung carcinoma, and cancers of the brain, kidney and breast in an NCI screen. Furthermore, compounds **14e** and **20** inhibit tubulin polymerisation and are not vulnerable to the overexpression of resistance conferring P-gp efflux pumps in drug-resistant breast cancer cells (NCI^{ADR/RES}). We also conducted X-ray crystallography studies that yielded the high-resolution structure of **14e** bound to tubulin. Our structural analysis revealed the key interactions between this noscapinoid and tubulin and will assist with the future design of noscapine derivatives with improved properties.

Introduction

The clinical success of tubulin-binding agents over the past few decades has made microtubules (MT) one of the most attractive molecular targets for the treatment of cancer. The potent anti-proliferative effects of these drugs are due to their interference

with MT dynamics, subsequently inducing cancer cell arrest at different phases of the cell division cycle.^[1] Nature has been one of the greatest sources of chemotherapeutics currently in clinical use.^[2,3] A large majority of tubulin-targeting agents are either directly derived from natural sources or generated through manifestation of nature-derived structures. These clinical agents either inhibit tubulin assembly (e.g., vinca alkaloids, colchicine) or inhibit MT disassembly (e.g., paclitaxel, epothilones).^[4] The development of chemoresistance has led to the downfall of these tubulin-targeted anti-cancer agents^[5] and many of these agents are also associated with several toxicity issues, including neuropathy.^[4] Thus, there is undoubtedly a demand for novel tubulin-binding agents that are devoid of these side effects.

Noscapine (**1**, Figure 1), a naturally-occurring phthalideisoquinoline alkaloid constituting 1–10% of alkaloid content in the opium poppy, *Papaver somniferum*, was found to inhibit tubulin polymerisation.^[6] Noscapine exhibited cytotoxic activities of 25, 39 and 42 μ M against cervical (HeLa), bladder (Renal 1983) and breast (MCF-7) cancers, respectively. Further evaluation studies showed that noscapine significantly inhibits the progression of tumour growth with low toxicity in surrounding healthy tissues.^[7] Noscapine was previously used as a clinical antitussive agent with an oral bioavailability of 30% and half-life of 4.5 h, thereby demonstrating an excellent safety and pharmacokinetic profile.^[8,9] Our research group has recently shown that the efficacy of noscapine was not reduced by the multidrug

[a] Dr. C. Yong, Dr. S. M. Devine,⁺ Dr. S. D. Tomlins, Prof. B. Capuano, Prof. P. J. Scammells
Medicinal Chemistry
Monash Institute of Pharmaceutical Sciences
Monash University
Parkville, VIC 3052 (Australia)
E-mail: peter.scammells@monash.edu
ben.capuano@monash.edu

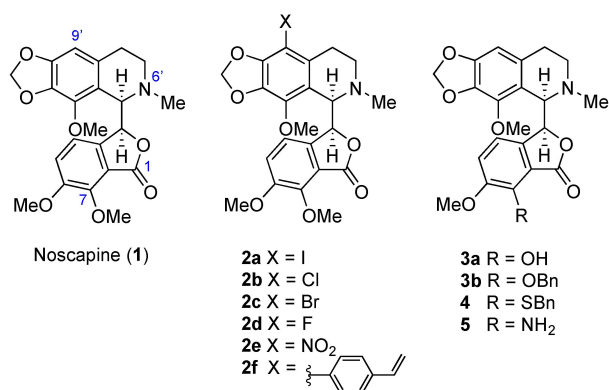
[b] A.-C. Abel,⁺ Prof. M. O. Steinmetz, Dr. A. E. Prota
Laboratory of Biomolecular Research,
Division of Biology and Chemistry
Paul Scherrer Institut
5232 Villigen PSI (Switzerland)
E-mail: andrea.prota@psi.ch

[c] Dr. D. Muthiah, X. Gao, Prof. R. Callaghan
Research School of Biology
Australian National University
Canberra, ACT 2061 (Australia)

[d] Prof. M. O. Steinmetz
Biozentrum
University of Basel
4056 Basel (Switzerland)

[⁺] These authors contributed equally to this work.

Supporting information for this article is available on the WWW under <https://doi.org/10.1002/cmdc.202100363>

Figure 1. Noscaphine (1) and noscapinoids 2–5.^[14–24]

resistant phenotype.^[10–12] Further investigation revealed noscaphine's inhibitory effects on P-glycoprotein (P-gp) through direct interaction with the transporter.^[13]

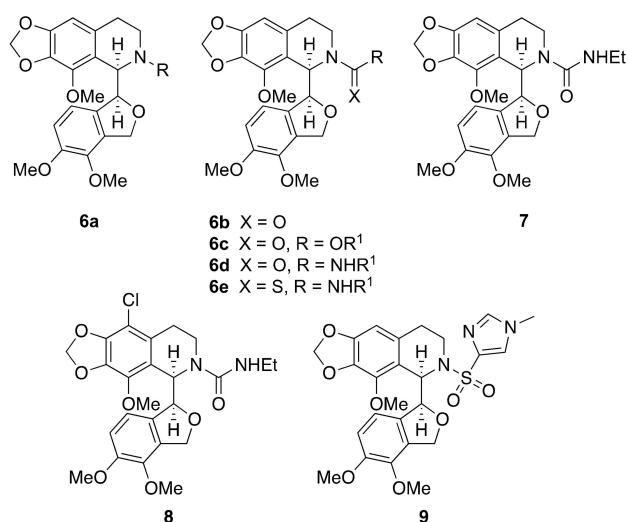
In the past two decades, many researchers have explored modifications at the 1, 7, 6' and 9'-positions of noscaphine, in search of more potent noscaphine analogues. The manipulation at the C9'-position was first explored with halo-substitution (Figure 1), where the analogues exhibited tubulin-binding activities greater than noscaphine (1) in the following order of magnitude: 9'-iodo (2a) > 9'-chloro (2b) > 9'-bromo (2c) > 9'-fluoronoscaphine (2d).^[14,15] This position was further explored with several nitrogen-containing functional groups such as -NO₂, -NH₂ and -N₃, where 9'-nitronoscaphine (2e) demonstrated anti-cancer activity against ovarian cancer cells (1A9) and drug-resistant ovarian cancer cells (1A9/PTX22) of 30.1 and 27.5 μM, respectively.^[16–18] A novel series of 9'-aryl noscapinoids were assessed and 9'-(4-vinylphenyl)noscaphine (2f) was shown to inhibit triple-negative breast cancer cells (MDA-MB-231) with an IC₅₀ of 6 μM.^[19]

The development of structure-activity relationships (SAR) at the southern isobenzofuranone ring have also been investigated by various research groups. This work was first conducted by Anderson *et al.*, where a regioselective O-demethylation was conducted at the C7-position.^[20] Following the discovery of 7-hydroxy noscaphine derivative 3a, a number of functional groups were explored at the C7-position (Figure 1). This includes O-acyl, O-benzyl, O-aryl, S-benzyl and 7-aminonoscaphine derivatives.^[21–23] The 7-hydroxy and 7-aminonoscaphine derivatives (3a and 5, respectively) caused the arrest of cells at the G₂/M phase at approximately 500 times increased potency in contrast with noscaphine (1). Compound 5 displayed a potency (IC₅₀) to inhibit proliferation of 94.3 and 237.4 nM against SNU398 and PLC/PRF/5 cells, respectively.^[24] Moreover, 5 was found to inhibit tubulin assembly with a tubulin-binding affinity of $1.1 \times 10^5 \text{ M}^{-1}$ at 25 °C. Despite its outstanding anti-mitotic profile, microsomal and S9 stability data suggests that 5 has high *in vivo* clearance. More recently, a new pro-drug hypothesis was introduced based on a high-resolution crystal structure of 7-aminonoscaphine (5),^[25] which proposed that

noscaphine would only bind to tubulin after metabolic oxidation and demethylation at the 7-position.

As part of our SAR investigation at the 6'-position of noscaphine, we have previously reported the synthesis and pharmacological evaluation of N-substituted cyclic ether noscaphine derivatives (6a–e) against breast (MCF-7), colon (Caco-2) and prostate (PC3) cancer cells (Figure 2).^[26] Several compounds from this focussed library showed potencies of $\leq 10 \mu\text{M}$. The replacement of N-methyl for longer N-alkyl chains (6a) was found to be detrimental to activity. N-Acyl (6b) and N-alkoxycarbonyl analogues (6c) with phenyl and benzyl substitution resulted in moderate mitotic arrest activity. Most notably, N-carbamoyl (6d) and N-thiocarbamoyl (6e) derivatives with short side chains displayed promising anti-mitotic activity. The cyclic ether N-ethylcarbamoyl noscaphine analogue 7 was found to be most active within this library, with EC₅₀ values of 3.6 μM and 6.7 μM against MCF-7 and PC3 cells, respectively.^[26] The inclusion of a 9-chloro group gave a further boost in potency with compound 8 exhibiting IC₅₀ values of 1.7 μM and 1.5 μM against MCF-7 and PC3 cells, respectively.^[10] We have also recently disclosed the replacement of N-methyl with an (N-methylimidazol-4-yl)sulfonyl moiety (9) at the N6'-position resulted in a 64-fold potency increase relative to noscaphine (1).^[12] Noscapinoid 9 possesses sub-micromolar activity against a range of cell lines (EC₅₀ values: 560 nM against MCF-7 cells; 980 nM against PANC-1 cells; 271 nM against MDA-MB-435 cells; 443 nM against SK-MEL-5 cells). Unlike many clinical anti-cancer agents, this potency is also maintained against drug-resistant NCI/AdR^{RES} cells, evidence of circumvention of common efflux mechanisms. Furthermore, 9 demonstrated a strong MT destabilising profile, where the rate of tubulin polymerisation was significantly reduced by 8-fold.

Though noscaphine has been the subject of extensive research, a region of the molecule that has remained unexplored is the 1,3-benzodioxole functionality. This motif is a common functionality found in natural products such as the

Figure 2. N-Substituted noscaphine and multi-functionalised derivatives 6a–e and 7–9.^[12, 26]

terpenes, saffrole, benzyloquinoline and aporphine alkaloids.^[27] The 1,3-benzodioxole moiety can also be found in clinical agents such as stiripentol and paroxetine for the treatment of epilepsy and depression, respectively.^[28,29] The dioxolane ring is a substrate for the cytochrome P450 system, and is commonly metabolised to an acetal moiety, which subsequently undergoes hydrolytic or oxidative cleavage to give the catechol or carbene species, respectively.^[30,31] The resultant carbene species is known to form an irreversible coordination to cytochrome enzyme CYP2D6, leading to the inactivation of this enzyme.^[30,32] As CYP2D6 is an enzyme that is involved in the metabolism of numerous drugs which includes antihypertensive agents, β -blockers, antiarrhythmic drugs, and antidepressants, inhibition of CYP2D6 produces an unwanted reduction in clearance of these clinical agents.^[33]

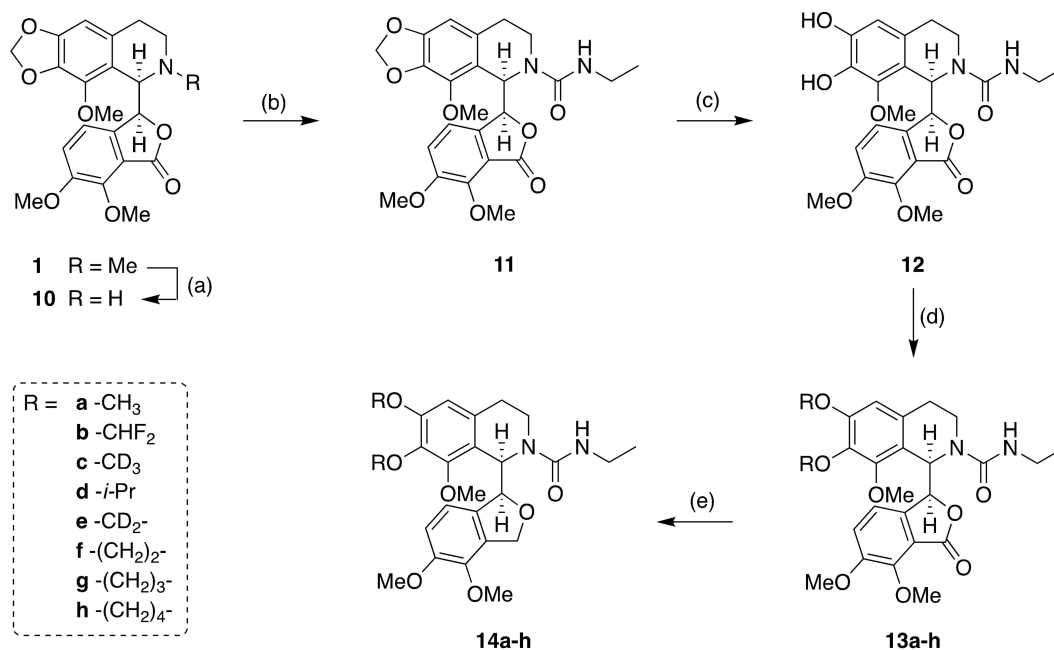
In this study, we have investigated a range of bioisosteres of the 1,3-benzodioxole motif present in noscapine in order to map the structure-activity relationships associated with this region of the molecule, identify more potent derivatives and potentially improve metabolic stability. The modifications include the replacement of the methylenedioxy group with dialkoxy substituents (including deuterium and fluorine containing alkoxy groups), the expansion of the dioxolane ring and the replacement of the hydrogens of the dioxolane ring with deuterium atoms. Herein, we report the synthesis and biological evaluation of a series of novel noscapine derivatives with a range of aforementioned modifications to the 1,3-benzodioxole functionality. These structural modifications were also combined with the modifications to the 1-, 6'- and 9'-positions that were previously shown to promote anti-proliferative activity. Finally, we determined the binding pose to

tubulin of one of these potent multi-functionalised noscapine derivatives to high resolution by X-ray crystallography. This crystal structure illuminated the observed SAR profile, most notably providing an explanation for poor activity of the noscapine derivatives with an unmodified lactone moiety relative to the series in which the lactone had been reduced to the desired cyclic ether.

Results and Discussion

Chemistry

The first steps in the synthesis of the targeted noscapine derivatives involved the preparation of *N*-ethylcarbamoyl noscapine (**11**) via *N*-demethylation of noscapine using an iron salt-mediated Polonovski reaction followed by reaction of the resultant secondary amine with ethyl isocyanate (Scheme 1). In order to introduce the proposed modifications to the 1,3-benzodioxole moiety of **11** the 1,3-dioxolane ring was subsequently cleaved to generate the corresponding catechol **12**. The ring was cleaved via a BCl_3 -mediated reaction, where the resultant complex (R-O-BCl_2) was hydrolysed in an acidic environment to give **12** in 95% yield. The subsequent alkylation reactions were achieved by treating the catechol **12** with the appropriate alkyl halide or dihalide and potassium carbonate. The only exception was the difluoromethoxy analogue **13b** which was prepared by treating **12** with sodium chlorodifluoroacetate and potassium carbonate. In the final step, the lactone moiety of compounds **13a-h** was reduced using $\text{NaBH}_4/\text{BF}_3\cdot\text{Et}_2\text{O}$



Scheme 1. Reagents and conditions: (a) (i) *m*-CPBA, CHCl_3 , 0 °C, 2 h, 95%, (ii) $\text{FeSO}_4\cdot 7\text{H}_2\text{O}$, MeOH, -5 °C, 1 h, 78%; (b) EtNCO , MeCN, 25 °C, 2 h, 84%; (c) BCl_3 , DCM, 25 °C, 16 h, 95%; (d) **13a**: MeI, K_2CO_3 , DMF, 81% **13b**: NaOOCF_2Cl , K_2CO_3 , DMF, 15%, **13c**: CD_3I , K_2CO_3 , DMF, 35%, **13d**: $(\text{CH}_3)_2\text{CHI}$, K_2CO_3 , DMF, 63% **13e**: CD_2I_2 , K_2CO_3 , DMF 42%, **13f-h**: $\text{Br}(\text{CH}_2)_n\text{Br}$, K_2CO_3 , DMF (14–60%); (e) $\text{NaBH}_4/\text{BF}_3\cdot\text{Et}_2\text{O}$, THF, 25 °C, 16 h, 6–75%.

to yield the corresponding cyclic ethers **14a–h** in yields ranging from 6 to 75%.

We have previously reported the benefits of installing a 9'-chloro group in combination with modifications to the 6'-position and reduction of the lactone of the isobenzofuranone.^[10] Accordingly we targeted the 9-chloro derivatives of the 1,4-dioxinotetrahydroisoquinoline **14f** as well as the corresponding analogue bearing a (*N*-methylimidazol-4-yl)sulfonyl moiety in the 6'-position. The synthesis of these compounds is shown in Scheme 2. Briefly, noscapine (**1**) was first converted to *N*-nornoscapine (**10**) via a non-classical Polonovski reaction.^[34,35] The secondary amine was then reacted with ethyl isocyanate or *N*-methylimidazolesulfonyl chloride to give **11** and **15**, respectively. Following previously described BCl₃-mediated conditions, the 1,3-dioxolane ring was then cleaved to give the catechols **12** and **16**, respectively. Installation of the 6-membered dioxane was conducted with K₂CO₃ and 1,2-dibromoethane, and the resultant products (**13f** and **17**) were chlorinated at the 9'-position using SO₂Cl₂ to afford **18** and **19**. Lastly, the lactone was reduced to the cyclic ether with a NaBH₄/BF₃·Et₂O system affording **20** and **21** in yields of 47% and 52%, respectively.

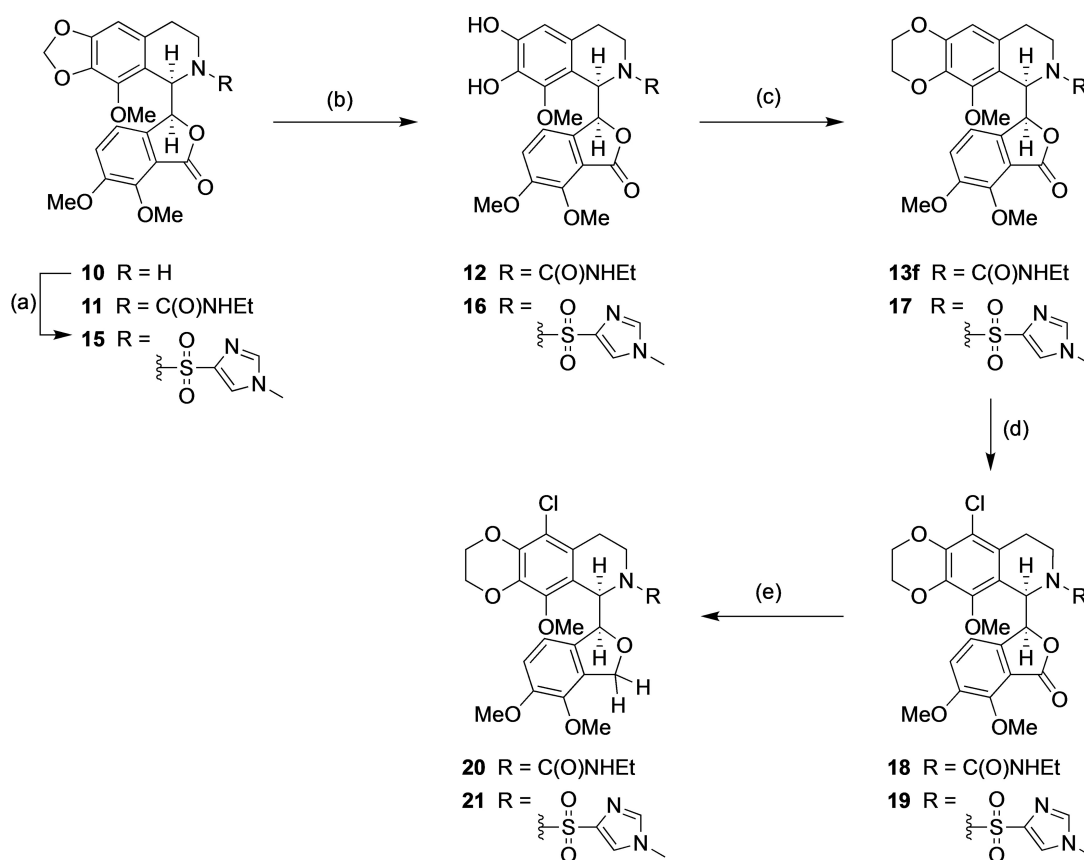
Biology

The impact of modification to the 1,3-dioxolane of noscapine on cell viability in cancer cells was determined by screening the noscapine analogues against breast (MCF-7) and pancreatic (PANC-1) cancer cells. Potent noscapinoids identified from the preliminary cell viability assay were then subjected to further assessment in tubulin polymerisation and resistance studies.

Cell viability assays

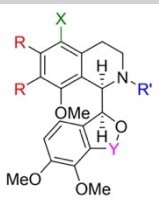
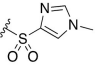
To assess the anti-proliferative impact of these noscapine derivatives, the compounds were subjected to cell viability studies against MCF-7 and PANC-1 cell lines. The MCF-7 and PANC-1 cells were treated with a broad range of concentrations (0.12–250 μM) of the noscapine analogues, and cell viability was determined at the conclusion of treatment using a resazurin-based assay (CellTiter-Blue®, Promega). EC₅₀ values were determined from the mean concentration-viability curves, in triplicate (n = 3), using GraphPad Prism v7.

A vast majority of these analogues, which includes the catechols **12** and **16** and the lactones **13a–h** and **17**, displayed low cytotoxic activities of >250 μM (Table 1), with the exception for **13e**, which displayed a potency of 94.4 ± 2.4 μM.



Scheme 2. Reagents and conditions: (a) *N*-methylimidazol-4-yl-SO₂Cl, Et₃N, DCM, 25 °C, 16 h, 82%; (b) BCl₃, DCM, 25 °C, 16 h, 82–95%; (c) Br(CH₂)₂Br, K₂CO₃, DMF, 25 °C or 80 °C, 16 h, 20–60%; (d) SO₂Cl₂, CHCl₃, 25 °C, 2 h, 31–75%; (e) NaBH₄/BF₃·Et₂O, THF, 25 °C, 16 h, 47–52%.

Table 1. Cell viability of noscapine derivatives.

						
Cpd No.	R	R'	Y	X	EC ₅₀ [μM] ^[a] MCF-7	PANC-1
1 ¹²	–OCH ₂ O–	–CH ₃	C=O	H	35.9 ± 0.1	19.3 ± 0.1
13a	–OCH ₃	–C(O)NH ₂	C=O	H	> 250	> 250
13b	–OCHF ₂	–C(O)NH ₂	C=O	H	> 250	> 250
13c	–OCD ₃	–C(O)NH ₂	C=O	H	> 250	> 250
13d	–O- <i>i</i> Pr	–C(O)NH ₂	C=O	H	> 250	> 250
13e	–OCD ₂ O–	–C(O)NH ₂	C=O	H	94.4 ± 2.4	> 250
13f	–O(CH ₂) ₂ O–	–C(O)NH ₂	C=O	H	> 250	> 250
13g	–O(CH ₂) ₃ O–	–C(O)NH ₂	C=O	H	> 250	> 250
13h	–O(CH ₂) ₄ O–	–C(O)NH ₂	C=O	H	> 250	> 250
7 ³⁰	–OCH ₂ O–	–C(O)NH ₂	CH ₂	H	3.6 ± 0.4	nd
14a	–OCH ₃	–C(O)NH ₂	CH ₂	H	28.9 ± 1.5	72.7 ± 1.9
14b	–OCHF ₂	–C(O)NH ₂	CH ₂	H	73.1 ± 1.4	65.3 ± 1.5
14c	–OCD ₃	–C(O)NH ₂	CH ₂	H	49.3 ± 1.9	2.5 ± 0.2
14d	–O- <i>i</i> Pr	–C(O)NH ₂	CH ₂	H	> 250	> 250
14e	–OCD ₂ O–	–C(O)NH ₂	CH ₂	H	1.5 ± 0.1	4.1 ± 0.2
14f	–O(CH ₂) ₂ O–	–C(O)NH ₂	CH ₂	H	12.5 ± 1.9	7.9 ± 1.4
14g	–O(CH ₂) ₃ O–	–C(O)NH ₂	CH ₂	H	28.5 ± 1.4	28.2 ± 1.6
14h	–O(CH ₂) ₄ O–	–C(O)NH ₂	CH ₂	H	34.3 ± 1.4	28.2 ± 1.6
20	–O(CH ₂) ₂ O–	–C(O)NH ₂	CH ₂	Cl	0.73 ± 0.1	1.1 ± 0.1
21	–O(CH ₂) ₂ O–		CH ₂	Cl	17.3 ± 1.6	3.8 ± 0.1

[a] Cell viability was determined using standard resazurin reduction method with CellTiter-Blue assay. EC₅₀ values shown represent the mean ± SEM for at least 3 independent observations.

In contrast, the reduction of these lactones to *N*-ethylcarbamoyl cyclic ether noscapine analogues (**14a–h**) led to significant improvements in potency (Table 1).

The observed cytotoxic activity of *N*-ethylcarbamoylnoscapine (**11**) was improved with the modification of 1,3-dioxolane to the dimethoxy (**14a**), bis-difluoromethoxy (**14b**), bis-trideuteriomethoxy (**14c**), 7-membered (**14g**) and 8-membered (**14h**) dioxacyclic *N*-ethylcarbamoyl noscapine analogues (EC₅₀ values: 28.5–73.1 μM). However, no cytotoxic activity was detected following bis-isopropyl replacements in **14d**. The results furnished that **14e**, whereby the naturally occurring methylene of the dioxolane ring in noscapine has been deuterated, displayed anti-cancer activities of 1.50 ± 0.1 μM and 4.1 ± 0.2 μM against MCF-7 and PANC-1 cells, respectively. Expansion to the 6-membered dioxane ring (**14f**) enhanced the anti-proliferative activity, with EC₅₀ values of 12.5 ± 1.9 μM in MCF-7 cell line and 7.9 ± 1.4 μM in PANC-1 cell line.

Introduction of a chloro substituent to **14f** at the 9'-position (**20**) further promoted cytotoxic activity (EC₅₀: 0.73 ± 0.1 μM against MCF-7 and 1.1 ± 0.1 μM against PANC-1), with a considerable 52-fold improvement in activity when contrasted with noscapine (**1**). This positive result further confirms the benefits with multi-functionalisation that was previously determined by DeBono *et al.*^[10] The anticipated potency gain with **21**, where *N*-ethylcarbamoyl in **14** was replaced with *N*-meth-

ylimidazol-4-ylsulfonyl, was instead met with a reduction of activity from **9** (EC₅₀: 17.3 ± 1.6 μM against MCF-7 and 3.8 ± 0.1 μM against PANC-1).

The noscapine derivative **20** was subjected to a further screening process against a panel of 60-cancer cell lines. This screening was performed by the Developmental Therapeutics Program, Division of Cancer Treatment and Diagnosis, National Cancer Institute (<http://dtp.cancer.gov>). Compound **20** was found to inhibit carcinoma cell growth with activities of > 2 μM against melanoma (MDA-MB-435), non-small cell lung (NCI-H522), CNS (SF-295) and renal (RXF) cancer lines (Figures S1 and S2). With a GI₅₀ value of 1.16 μM, **20** can be acknowledged as a potent growth inhibitor for MDA-MB-435. Compound **20** also displayed an exemplary cytotoxic potency, with an LC₅₀ of 79.8 μM against melanoma (SK-MEL-5) cells.

Cellular antiproliferative studies against sensitive- and resistant-cancer cells

The development of resistance towards chemotherapeutic agents is currently one of the major causes of treatment failure. A key mechanism of acquired resistance is the increased expression of P-gp, subsequently increasing the efflux of cytotoxic agents from the cytoplasm of the cell.^[36] To determine if the promising anti-proliferative activity of compounds **14e** and **20** is affected by the overexpression of P-gp, the ability of **20** to inhibit proliferation in the drug-sensitive MCF-7^{WT} breast cancer cell line and its drug-resistant variant, the NCI^{ADR/RES} cancer cell line (high P-gp expression levels) was assessed. The clinical anti-mitotic agent, vinblastine, displayed an EC₅₀ of 0.24 ± 0.04 nM in MCF-7^{WT} cells and 33.1 ± 7.3 nM in NCI^{ADR/RES} cells (Table 2).

The statistically significant (*p* < 0.05, *n* = 8) 138-fold difference in potency between the drug-sensitive and resistant cells confirmed that vinblastine was affected by the MDR phenotype exhibited by the NCI^{ADR/RES} cells. Conversely, noscapine (**1**) demonstrated anti-proliferative activities of 13.7 ± 3.0 μM and 24.7 ± 3.5 μM against MCF-7^{WT} and NCI^{ADR/RES} cells, respectively. Although there was a statistically significant difference in noscapine potency between the two cell lines (*p* < 0.05), the degree of resistance was a modest 1.8-fold, which is consistent

Table 2. Cell proliferation of Vinblastine, Noscapine (**1**), **14e** and **20** in drug-sensitive (MCF-7^{WT}) and -resistant (NCI^{ADR/RES}) breast cancer cell lines

Cpd No.	EC ₅₀ [μM] ^[a] MCF-7 ^{WT}	NCI ^{ADR/RES}	Fold Ratio
Vinblastine ^[b]	0.24 ± 0.04	33.1 ± 7.3	138
Noscapine (1)	13.7 ± 3.0	24.7 ± 3.5	1.8
14e	1.6 ± 0.1	1.5 ± 0.1	0.94
20	0.65 ± 0.17	0.81 ± 0.21	1.2

[a] Cells were treated with varying concentrations of test compounds, and cell viability was determined using a standard MTT assay. Potency was determined by nonlinear least-squares regression of the sigmoidal dose – response equation. The data represent the means ± SEM for at least eight independent observations. [b] The EC₅₀ values for vinblastine are in nanomolar (nM).

with previous findings and markedly lower than observed for vinblastine.^[10–12] Compound **14e** was found to be equipotent in the drug-sensitive and resistant cell lines, with EC_{50} values of $1.6 \pm 0.1 \mu\text{M}$ and $1.5 \pm 0.1 \mu\text{M}$, respectively. A similar outcome was observed for **20**, with EC_{50} values of $0.65 \pm 0.17 \mu\text{M}$ and $0.81 \pm 0.21 \mu\text{M}$ against drug-sensitive and the resistant cells, respectively. This indicates that the overexpression of P-gp in the drug-resistant NCI^{ADR/RES} does not alter the efficacies of noscapine (**1**), **14e** or **20**. Therefore, the noscapine derivatives **14e** and **20** are not susceptible to the common MDR phenotype that many clinical anti-mitotic agents are vulnerable to, including vinblastine.

Inhibitory effects on tubulin polymerisation

The effectiveness in tubulin-targeting agents currently used in cancer treatments are due to their ability to disrupt MT dynamics through binding to tubulin, subsequently triggering apoptotic mechanisms of the affected carcinoma.^[1] As a MT-destabilising agent, noscapine (**1**) was previously found to reduce the maximum initial velocity (V_{max}) of tubulin polymerisation in a concentration-dependant manner.^[6] This inhibitory action has also been consistently observed across the years by various noscapine research groups.^[11,12,24,37] The key compounds of this series, **14e** and **20**, were evaluated for their capacity to inhibit tubulin polymerisation.

Tubulin polymerisation was induced with GTP, followed by addition of ligands at $10 \mu\text{M}$. Fluorescence intensities were measured at 1-minute intervals across a period of 60 minutes, with the temperature maintained at 37°C throughout the experiment. The control ($V_{\text{max}} = 24.5 \pm 1.2 \text{ mOD/min}$) represents a classic polymerisation curve in the absence of tubulin ligands (Figure 3). Paclitaxel produced a conventional MT-stabilising polymerisation curve, whereby a three-fold increase in V_{max} was observed ($V_{\text{max}} = 70.7 \pm 6.2 \text{ mOD/min}$). In contrast, noscapine (**1**) instigated a reduction of V_{max} to a polymerisation rate of $18.1 \pm 1.0 \text{ mOD/min}$. The novel noscapine analogues, **14e** and **20**, inhibited tubulin polymerisation to V_{max} rates of $12.0 \pm 0.8 \text{ mOD/min}$ and $1.9 \pm 0.03 \text{ mOD/min}$, respectively. These results confirmed that **14e** and **20** both bind to tubulin, and like

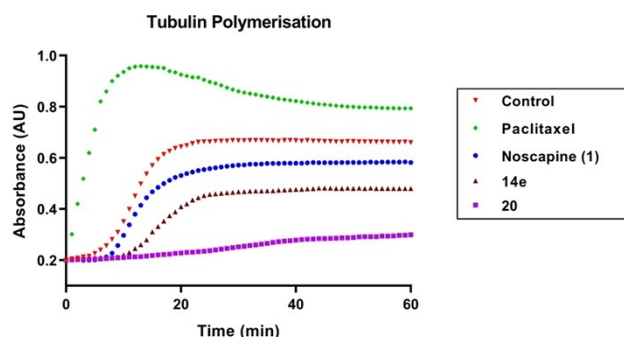


Figure 3. Polymerisation of porcine brain derived tubulin dimers in the absence (▼) and presence of ligands (paclitaxel, ◆; noscapine (**1**), ●; **14e**, ▲; **20**, ■).

noscapine (**1**), the anti-proliferative effect observed against MCF-7 cells is likely due to interference with MT dynamics. Apart from the significant 13-fold reduction in V_{max} , **20** remained in the growth phase of the polymerisation curve over the course of the 60-minute experiment. Given that the other tubulin ligands, paclitaxel, noscapine (**1**) and **14e**, reached a steady state at $t = 25 \text{ min}$ onwards, this result indicates that **20** possesses a strong inhibitory effect on tubulin polymerisation.

X-ray crystallography

Crystal structure of the tubulin-compound 14e complex. To support the SAR of **14e** and to define its interaction mode with tubulin, we sought to determine the crystal structure of the compound in complex with tubulin by X-ray crystallography. To this end, we soaked **14e** in a crystal formed by a protein complex composed of two $\alpha\beta$ -tubulin heterodimers, the stathmin-like protein RB3 and tubulin tyrosine ligase (T_2R -TTL).^[38,39] We solved the crystal structure of T_2R -TTL-**14e** at a resolution of 2.2 \AA (Table S1).

Compound **14e** binds to the colchicine site of tubulin, which is formed by residues of the $\alpha T5$ loop of α -tubulin together with residues of strands $\beta S8$, $\beta S9$, $\beta S10$, helices $\beta H7$ and $\beta H8$ and loop $\beta T7$ of β -tubulin (PDB ID: 7AU5) (Figure 4). We determined the occupancy of compound **14e** at 75% within the colchicine site of $\alpha\beta$ -tubulin (chains A and B of T_2R -TTL) (Figure S2). In addition, the observed binding mode is in accord with the one recently published for the closely related 7-aminonoscapine.^[25] Superimposition of the tubulin structure in the absence of any ligand^[38] with the T_2R -TTL-**14e** structure suggests that binding of compound **14e** has no impact on the overall T_2R -TTL structure (PDB ID: 4I55, overall $\text{rmsd}_{T_2R\text{-TTL-17e}}$ of 0.30 \AA over 2072 C_α -atoms; chain B: $\text{rmsd}_{T_2R\text{-TTL-17e}}$ of 0.18 \AA over 378 C_α -atoms).

The main interactions between tubulin and compound **14e** are via hydrogen bonds and electrostatic interactions. The tetrahydro[1,3]dioxolo[4,5-*g*]isoquinoline ring (Figure 4B) of **14e** is stacked between helices $\beta H7$ and $\beta H8$, specifically between the residues $\beta Cys342$ and $\beta Leu255$ (Figure 4B,C). Furthermore, the residues $\beta Tyr202$, $\beta Val238$, $\beta Leu242$, $\beta Leu255$, $\beta Ile318$, $\beta Ile378$ form a pocket for coordination of the 1,3-dioxolo moiety containing the deuterated methylene group. The oxygen of the 4-methoxy group forms a hydrogen bond to the main chain amide of $\beta Ala250$, whereas the methyl group engages in a hydrophobic contact to $\beta Leu242$.

The 4,5-dimethoxy-1,3-dihydroisobenzofuran ring is positioned at the $\alpha\beta$ -tubulin heterodimer interface and rests between the helix $\beta H8$ and the $\alpha T5$ loop. The residue $\beta Met259$ ($\beta H8$ helix), the amino-terminal end of the strand $\beta S9$ and the side chain of $\alpha Val181$ ($\alpha T5$ -loop) together form a cavity in which the 6-methoxy group is coordinated. The oxygen of the 7-methoxy group is involved in a weak polar interaction (4.3 \AA distance) with the main chain amide of $\alpha Val181$. Lastly, the *N*-ethylcarbamoyl group at the *N6'*-position is oriented towards the nucleotide with the carbonyl facing the $\beta S9$ strand. The

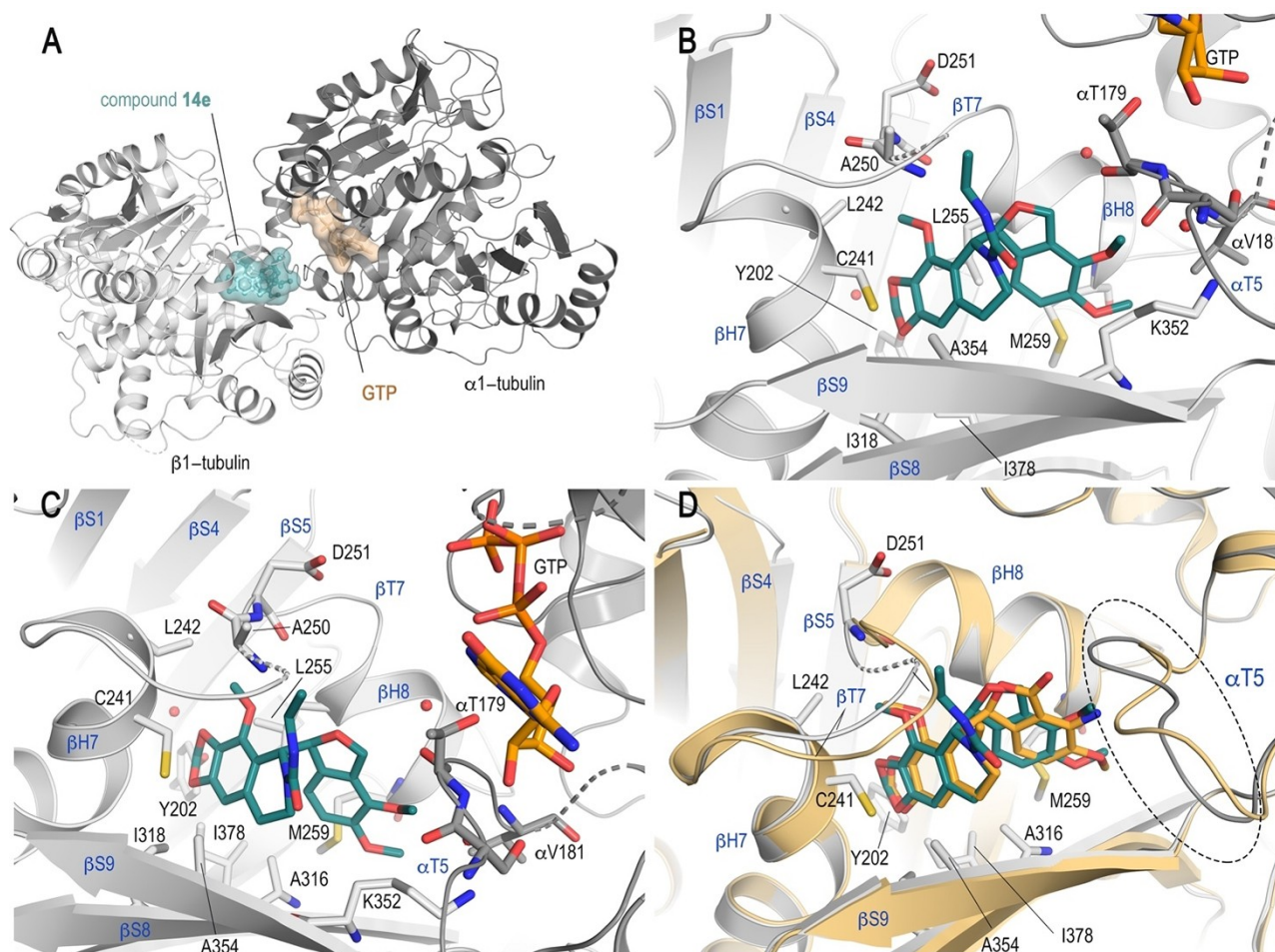


Figure 4. Tubulin-14e complex structure (PDB ID: 7AU5) and superposition with the tubulin-7-aminonoscapine structure; (A) Overview of compound 14e bound to the colchicine site in α -tubulin (chains A and B of T₂R-TTL). Ribbon representations of the α - and β -tubulin chains are coloured in dark and light grey, respectively. Compound 14e (light blue) and the GTP molecule (light orange) are displayed in stick and surface representation. All carbon atoms are coloured according to their chain assignment; oxygen atoms and nitrogen atoms are coloured red and blue, respectively. (B), (C) Two close-up views of the compound 14e (cyan) binding mode. Interacting tubulin residues are labelled and shown in stick representation; α -tubulin residues are specifically labelled as such. Secondary structural elements are labelled in blue. Water molecules are shown as red spheres and hydrogen bonds are indicated by black-dashed lines. The GTP molecule (orange) is shown in stick representation and the disordered segment of the β -tubulin T7 loop is displayed as a dashed line. (D) Superposition of the T₂R-TTL-7-aminonoscapine structure (PDB ID: 6Y6D, yellow) and the T₂R-TTL-14e structure (tubulin in grey, 14e in cyan). Both ligands as well as interacting tubulin residues are displayed in stick representation. The shown tubulin residues are labelled and α -tubulin residues are specifically labelled as such. Oxygen and nitrogen atoms are coloured red and blue, respectively. Secondary structural elements are labelled in blue; hydrogen-bonds are displayed as black dashed lines. A dashed ellipse is centred around the α -tubulin α T5 loop to highlight the two observed conformations.

contained ethyl group displaces residue β Leu249, thereby causing disorder of this segment of the β T7 loop.

Comparison between 14e and 7-aminonoscapine (5). To date, only one high-resolution crystal structure for noscapine derivatives has been published,^[25] introducing the hypothesis that the parental noscapine is a pro-drug. Here, we show that compound 14e is able to bind to tubulin, despite containing the critical 7-methoxy moiety. Hence, we superimposed our crystal structure to the T₂R-TTL-7-aminonoscapine one (Figure 4D) to investigate the differences in the compound binding modes.

Superimposition of the T₂R-TTL-7-aminonoscapine structure with the T₂R-TTL-14e structure shows only very small deviations at an overall structural level (PDB ID: 6Y6D, overall: rmsd_{T₂R-TTL-7-aminonoscapine} 0.23 Å over 1989 C $_{\alpha}$ atoms, chain B: rmsd_{T₂R-TTL-7-aminonoscapine} 0.20 over 370 C $_{\alpha}$ atoms). Since the

tetrahydro[1,3]dioxolo[4,5-g]isoquinoline moiety of both molecules is identical, except for the deuterated bridging methylene moiety in 14e, coordination of this ring system occurs in the same manner in both complexes.

Interestingly, in the T₂R-TTL-7-aminonoscapine structure the α T5 loop is flipped at α Thr179 compared to the apo-T₂R-TTL structure. This reorganisation takes place to enable water mediated hydrogen bonds with the carbonyl group of 7-aminonoscapine. As this carbonyl group is reduced to a methylene in compound 14e, the flip of the α T5 loop does not occur in the T₂R-TTL-14e structure. Furthermore, this allows the whole dihydroisobenzofuran moiety of 14e to rest closer to the dioxolo-tetrahydroisoquinoline group at the centre of the colchicine site compared to its position in the tubulin-7-aminonoscapine complex. This repositioning prevents clashes

of the 7-methoxy group with the α T5 loop that hinder binding of the parental compound noscapine and thus enables binding of **14e** despite the presence of the same 7-methoxy group.

The *N*-ethylcarbamoyl group is oriented as the *N*6'-methyl group in the 7-aminonoscapine structure towards the nucleotide and the β T7 loop. In the 7-aminonoscapine structure, a flip in the β T7 loop, compared to the apo position is sufficient to accommodate the *N*6'-methyl group. However, this flip is not sufficient to accommodate the elongated *N*-ethylcarbamoyl moiety in **14e**. As a consequence, it displaces both the residues β Asn249 and β Leu249, and causes them to remain unresolved in the structure.

Both **14e** and 7-aminonoscapine adopt a similar pose within the colchicine site, suggesting a common mechanism to perturb MTs. The higher impact of **14e** on the overall organization of the binding site could explain the higher potency of the ligand compared to noscapine. The reduction of the 1-carbonyl group in compound **14e** enables the α T5 loop to coordinate the compound closer to the centre of the binding site and thereby enables accommodation of the 7-methoxy group, which is predicted to hinder noscapine binding.^[25]

Conclusion

A series of 1,3-benzodioxole modified noscapine analogues were synthesised to allow for the novel SAR exploration at this region of the noscapine scaffold. The tubulin inhibitory profile and anti-cancer activities of these compounds were evaluated in comparison to noscapine (**1**), with the natural 1,3-benzodioxole group in place. The lack of anti-proliferative activity against MCF-7 and PANC-1 cells in lactone analogues **13a–h** were recovered following reduction to its respective cyclic ether *N*-ethylcarbamoyl noscapine derivatives **14a–h**. The isosteric replacement of the hydrogens of the methylenedioxy bridge with deuterium (**14e**) resulted in a 25-fold increase in potency (EC_{50} : $1.5 \pm 0.1 \mu\text{M}$) against MCF-7 cells, relative to that of noscapine (**1**). Compound **14e** was also found to inhibit tubulin polymerisation to a rate of $12.0 \pm 0.8 \text{ mOD/min}$. This preference for the deuterium over hydrogen indicates that substitution at the 2'-methylene position is tolerated within this region of the tubulin-binding site. Our research efforts to form the second generation of multi-functionalised noscapine derivatives afforded **20** as a potent tubulin polymerisation inhibitor (V_{max} : $1.9 \pm 0.04 \text{ mOD/min}$). Compound **20** instigated a 13-fold reduction in tubulin polymerisation rate relative to the DMSO control. Furthermore, **20** exhibited pronounced cytotoxic activity of $0.73 \pm 0.1 \mu\text{M}$ and $1.1 \pm 0.1 \mu\text{M}$ against MCF-7 and PANC-1 cells, respectively. Screening against a panel of 60-cancer cell lines conducted by the NCI revealed that **20** was also active against MDA-MB-435, NCI-H522, SF-295 and RXF cells, with activities of $> 2 \mu\text{M}$. Compound **20** was particularly active against melanoma cells, with GI_{50} of $1.16 \mu\text{M}$ and LC_{50} of $79.8 \mu\text{M}$ against MDA-MB-435 and SK-MEL-5, respectively. More importantly, both compounds **14e** and **20** maintain their potency in the drug-resistant NCI^{ADR/RES} cell line, an indication

that these noscapine derivatives are not susceptible to the common MDR phenotype.

Furthermore, structural studies yielded a crystal structure of **14e** bound to tubulin, which revealed that it binds to the colchicine site of tubulin. This structural study pinpointed the key interactions between **14e** and tubulin as well as its binding mode relative to the only other reported high-resolution crystal structure of a noscapine derivative (7-aminonoscapine) bound to tubulin. The structural studies of noscapine derivatives in complex with tubulin may eventually enable the rational design of this class of anti-tubulin compounds with the aim to produce further variants with superior pharmacological profiles.

Experimental Section

Chemistry

NMR spectra (^1H , ^{19}F and ^{13}C) were recorded on a Bruker Avance Nanobay III 400 MHz Ultrashield Plus spectrometer at 400.13, 376.85 and 100.62 MHz, respectively coupled to a BACS 60 automatic sample changer at 25 °C. Chemical shifts (δ) are recorded in parts per million (ppm) by correction with reference to the chemical shift of the solvent. Coupling constants (*J*) are recorded in Hz, and the significant multiplicities described by singlet (s), doublet (d), triplet (t), quadruplet (q), broad (br), multiplet (m), doublet of doublets (dd), and doublet of triplets (dt). LC–MS were run on an Agilent 6120 series Single Quad coupled to an Agilent 1260 series HPLC. The following buffers were used: buffer A, 0.1% formic acid in H_2O ; buffer B, 0.1% formic acid in MeCN. The following gradient was used with a Phenomenex Luna 3 μM C8(2) 15 mm \times 4.6 mm column, and a flow rate of 0.5 mL/min and total run time of 12 min; 0–4 min 95% buffer A and 5% buffer B, 4–7 min 0% buffer A and 100% buffer B, 7–12 min 95% buffer A and 5% buffer B. Mass spectra were acquired in positive and negative ion mode with a scan range of 0–1000 *m/z* at 5 V. UV detection was carried out at 214 nm and 254 nm. All screening compounds were of $> 95\%$ purity.

Analytical HPLC was performed using an Agilent 1260 Infinity Analytical HPLC with a Zorbax Eclipse Plus C18 Rapid Resolution 4.6 \times 100 mm, 3.5 μM column. Buffer A: 0.1% TFA in H_2O and buffer B: 0.1% TFA in MeCN were used. Samples were run at a gradient of 30% buffer B/ buffer A (0–5 min) to 100% buffer B (5–6 min) at a flow rate of 1 mL/min. Unless otherwise indicated, all compounds were $> 95\%$ by HPLC prior to biological evaluation. Thin layer chromatography was conducted on 0.2 mm plates using Merck silica gel 60 F_{254} . Column chromatography was achieved using Merck silica gel 60 (particle size 0.063–0.200 μm , 70–230 mesh).

General Procedure A: 1,3-Dioxolane Ring Cleavage. To a stirring solution of **11** or **15** (1.0 eq) in DCM (50 mL), was added BCl_3 (1 M in DCM, 2.0 eq) and the mixture stirred at 25 °C for 16 h. The reaction was quenched with MeOH (50 mL) and the solvent was removed *in vacuo*. The resultant solid was then stirred in 1 M HCl (20 mL) at 90 °C for 30 min. The mixture was basified to pH 8 with sat. NaHCO_3 and precipitation was observed. The suspension was filtered to afford the desired catechol (**12** or **16**).

General Procedure B: Catechol Alkylation. To a solution of **12** or **16** (1.0 eq) in DMF (2 mL) was added K_2CO_3 or NaOH, and the mixture was left to stir at 25 °C for 5 min. The appropriate alkylating agent was added and the reaction was stirred at the described conditions. The resultant mixture was then pipetted over ice and precipitation was observed. The suspension was filtered to yield the crude

product. The crude residue was purified by flash chromatography (1:1; EtOAc:pet. spirits) to afford the title products.

General Procedure C: Lactone Reduction. To a stirring solution of NaBH_4 (5.0 eq) in THF at -5°C , was added **13a–h**, **18** or **19** (1.0 eq) dissolved in $\text{BF}_3\cdot\text{Et}_2\text{O}$ (39 eq) dropwise. The mixture was warmed to 25°C and stirred for 16 h. The reaction was quenched with 10% aq. HCl and stirred for 1 h. The solution was extracted with CHCl_3 (3 \times). The combined organic layers were washed with 10% aq. NaOH, dried with MgSO_4 , filtered and the solvent removed *in vacuo*. The crude product was then purified by flash chromatography (EtOAc) to yield the desired cyclic ether (**14a–h**, **20** and **21**).

(R)-5-((S)-4,5-Dimethoxy-3-oxo-1,3-dihydroisobenzofuran-1-yl)-N-ethyl-4-methoxy-7,8-dihydro[1,3]dioxolo[4,5-g]isoquinoline-6(5H)-carboxamide (11). To a cooled solution (-5°C) of **10** (353 mg, 0.886 mmol) in CH_3CN (15 mL) was added EtNCO (105 μL , 1.33 mmol). The reaction was warmed to 25°C and stirred for 2 h. The reaction was then concentrated *in vacuo* and H_2O (15 mL) was added to the resulting brown solid. The mixture was extracted with DCM (3 \times 15 mL), washed with sat. NaCl (20 mL), with the organic layer dried over anhydrous MgSO_4 , filtered and concentrated *in vacuo* to yield the crude product as a yellow foam. The crude product was then purified by flash column chromatography (EtOAc) to give the title product as a white foam (356 mg, 85%). ^1H NMR (d_6 -DMSO): δ 7.41 (d, $J=8.4$ Hz, 1H), 6.90 (d, $J=8.3$ Hz, 1H), 6.53 (s, 2H), 5.94 (d, $J=4.4$ Hz, 2H), 5.81 (d, $J=4.6$ Hz, 1H), 5.65 (d, $J=4.6$ Hz, 1H), 3.83 (s, 6H), 3.69 (s, 3H), 3.32–3.26 (m, 1H), 3.11–3.00 (m, 3H), 2.90–2.74 (m, 1H), 2.74–2.59 (m, 1H), 1.02 (t, $J=7.1$ Hz, 3H); ^{13}C NMR (d_6 -DMSO): δ 167.3, 157.8, 152.6, 148.6, 147.1, 141.0, 140.0, 134.2, 131.3, 120.1, 119.0, 118.3, 117.3, 103.0, 101.3, 81.6, 62.0, 59.4, 57.1, 55.4, 51.5, 35.5, 27.9, 16.1. HR-ESMS calcd. for $\text{C}_{24}\text{H}_{27}\text{N}_2\text{O}_8$ $^+$ [M + H] 471.1762, found 471.1771.

(R)-1-((S)-4,5-Dimethoxy-3-oxo-1,3-dihydroisobenzofuran-1-yl)-N-ethyl-6,7-dihydroxy-8-methoxy-3,4-dihydroisoquinoline-2(1H)-carboxamide (12). Compound **12** was synthesised from **11** (251 mg, 0.534 mmol) according to General Procedure A, with BCl_3 (1 M in DCM, 1.07 mL, 1.07 mmol). The product was obtained as a white foam (232 mg, 95%). ^1H NMR ($\text{DMSO}-d_6$): δ 9.27 (s, 1H), 8.40 (s, 1H), 7.32 (d, $J=8.4$ Hz, 1H), 6.57–6.44 (m, 2H), 6.38 (s, 1H), 5.76 (d, $J=5.1$ Hz, 1H), 5.73 (d, $J=5.0$ Hz, 1H), 3.84 (s, 3H), 3.81 (s, 3H), 3.68 (s, 3H), 3.47–3.37 (m, 2H), 3.05 (s, 2H), 2.53–2.49 (m, 2H), 1.01 (t, $J=7.1$ Hz, 3H); ^{13}C NMR (CDCl_3): δ 167.4, 157.9, 152.6, 147.3, 146.6, 145.7, 141.0, 136.5, 126.6, 119.9, 118.7, 118.6, 116.2, 110.9, 80.8, 62.0, 60.2, 57.0, 51.3, 35.5, 27.2, 16.1. HR-ESMS calcd. for $\text{C}_{23}\text{H}_{27}\text{N}_2\text{O}_8$ $^+$ [M + H] 459.1762, found 459.1769.

(R)-1-((S)-4,5-Dimethoxy-3-oxo-1,3-dihydroisobenzofuran-1-yl)-N-ethyl-6,7,8-trimethoxy-3,4-dihydroisoquinoline-2(1H)-carboxamide (13a). Compound **13a** was synthesised from **12** (1.30 g, 2.84 mmol) according to General Procedure B, with NaOH (340 mg, 8.52 mmol) and iodomethane (583 μL , 9.36 mmol). The aqueous layer was extracted with EtOAc (3 \times 25 mL) and solvent removed *in vacuo* to yield the crude product. The product was purified with flash column chromatography (1:1; EtOAc; pet. spirits) and obtained as a pale yellow foam (1.12 g, 81%). ^1H NMR (CD_3OD): δ 7.29 (d, $J=8.3$ Hz, 1H), 6.78 (d, $J=8.1$ Hz, 1H), 6.61 (s, 1H), 5.88 (q, $J=3.9$ Hz, 2H), 3.90 (s, 3H), 3.86 (s, 3H), 3.83 (s, 3H), 3.78 (s, 3H), 3.68 (s, 3H), 3.50–3.40 (m, 1H), 3.29–3.20 (m, 2H), 2.87 (dt, $J=19.3$, 9.2 Hz, 2H), 2.77–2.64 (m, 1H), 1.16 (t, $J=7.2$ Hz, 3H); ^{13}C NMR (CD_3OD): δ 160.4, 154.7, 154.2, 151.5, 148.9, 141.6, 141.2, 141.2, 133.8, 120.7, 120.0, 119.5, 117.6, 108.3, 83.3, 62.4, 61.2, 57.3, 56.4, 53.6, 40.8, 36.9, 36.7, 29.0, 15.9. HR-ESMS calcd. for $\text{C}_{25}\text{H}_{31}\text{N}_2\text{O}_8$ $^+$ [M + H] 487.2075, found 487.2087.

(R)-6,7-Bis(difluoromethoxy)-1-((S)-4,5-dimethoxy-3-oxo-1,3-dihydroisobenzofuran-1-yl)-N-ethyl-8-methoxy-3,4-dihydroisoquinoline-2(1H)-carboxamide (13b). To a stirring solution of **12** (254 mg, 0.555 mmol), K_2CO_3 (307 mg, 2.22 mmol) and H_2O (40 μL , 2.22 mmol) in DMF (2 mL) was added sodium chlorodifluoroacetate (338 mg, 2.22 mmol). The mixture was heated to 80°C for 16 h, then cooled to 25°C and diluted with H_2O (10 mL). The aqueous phase was extracted with EtOAc (3 \times 15 mL) and the combined organic fractions were washed with H_2O (3 \times 10 mL), dried with MgSO_4 , filtered, and concentrated *in vacuo*. The crude material purified by flash chromatography (1:1; EtOAc:pet. spirits) give the title product as a colourless oil (47 mg, 15%). ^1H NMR (CDCl_3): δ 7.11 (d, $J=8.3$ Hz, 1H), 6.84 (d, $J=8.2$ Hz, 1H), 6.80 (s, 1H), 6.52 (dd, $J=73.2$, 73.2 Hz, 1H), 6.27 (dd, $J=75.3$, 73.8 Hz, 1H), 5.94 (d, $J=3.1$ Hz, 1H), 5.81 (d, $J=3.1$ Hz, 1H), 4.86 (t, $J=5.3$ Hz, 1H), 3.97 (s, 3H), 3.86 (s, 3H), 3.77 (s, 3H), 3.59–3.50 (m, 1H), 3.38–3.25 (m, 2H), 3.10–2.99 (m, 1H), 2.90–2.81 (m, 1H), 2.80–2.70 (m, 1H), 1.19 (t, $J=7.2$ Hz, 3H); ^{19}F NMR (CDCl_3): δ –81.05 (d, $J=164.0$ Hz), –81.29 (d, $J=162.6$ Hz), –81.68 (d, $J=164.0$ Hz), –82.35 (d, $J=162.6$ Hz); ^{13}C NMR (CDCl_3): δ 167.2, 158.5, 152.9, 150.7, 148.2, 144.0 (app t, $J=2.7$ Hz), 139.6, 136.5, 133.4 (app t, $J=3.3$ Hz), 122.6, 119.1, 118.5, 118.3, 116.7 (app t, $J=263.0$ Hz), 115.7 (app t, $J=263.0$ Hz), 115.6, 81.9, 62.4, 61.3, 57.0, 53.5, 39.5, 36.1, 28.2, 15.7. HR-ESMS calcd. for $\text{C}_{25}\text{H}_{27}\text{F}_4\text{N}_2\text{O}_8$ $^+$ [M + H] 559.1698, found 559.1709.

(R)-1-((S)-4,5-Dimethoxy-3-oxo-1,3-dihydroisobenzofuran-1-yl)-N-ethyl-8-methoxy-6,7-bis(methoxy- d_3)-3,4-dihydroisoquinoline-2(1H)-carboxamide (13c). Compound **13c** was synthesised from **12** (496 mg, 1.42 mmol) according to General Procedure B, with K_2CO_3 (747 mg, 5.40 mmol) and iodomethane- d_3 (168 μL , 2.70 mmol). The product was obtained as a white foam (188 mg, 35%). ^1H NMR (CDCl_3): δ 6.99 (d, $J=8.3$ Hz, 1H), 6.53 (d, $J=8.2$ Hz, 1H), 6.36 (s, 1H), 5.94 (d, $J=3.1$ Hz, 1H), 5.58 (d, $J=3.3$ Hz, 1H), 5.05 (t, $J=5.4$ Hz, 1H), 3.92 (s, 3H), 3.77 (s, 3H), 3.76 (s, 3H), 3.63–3.54 (m, 1H), 3.31–3.11 (m, 2H), 2.74–2.53 (m, 2H), 2.42–2.30 (m, 1H), 1.11 (t, $J=7.2$ Hz, 3H); ^{13}C NMR (CDCl_3): δ 167.1, 158.8, 153.0, 152.5, 149.9, 147.9, 139.9, 139.7, 132.3, 118.7, 118.3, 118.3, 115.8, 106.9, 81.4, 62.2, 60.6, 56.7, 53.6, 38.9, 35.8, 27.9, 15.5. HR-ESMS calcd. for $\text{C}_{25}\text{H}_{25}\text{D}_6\text{N}_2\text{O}_8$ $^+$ [M + H] 493.2452, found 493.2432.

(R)-1-((S)-4,5-Dimethoxy-3-oxo-1,3-dihydroisobenzofuran-1-yl)-N-ethyl-6,7-diisopropoxy-8-methoxy-3,4-dihydroisoquinoline-2(1H)-carboxamide (13d). Compound **13d** was synthesised from **12** (207 mg, 0.452 mmol) according to General Procedure B, with K_2CO_3 (313 mg, 2.26 mmol) and 2-iodopropane (136 μL , 1.36 mmol). The product was obtained as a white solid (154 mg, 63%). ^1H NMR ($\text{DMSO}-d_6$): δ 7.36 (d, $J=8.4$ Hz, 1H), 6.79 (d, $J=8.3$ Hz, 1H), 6.62 (s, 1H), 6.54 (t, $J=5.4$ Hz, 1H), 5.78 (d, $J=4.5$ Hz, 1H), 5.72 (d, $J=4.4$ Hz, 1H), 4.62–4.50 (m, 1H), 4.17–4.04 (m, 1H), 3.81 (s, 3H), 3.80 (s, 3H), 3.65 (s, 3H), 3.45–3.35 (m, 1H), 3.14–3.03 (m, 2H), 2.97–2.87 (m, 1H), 2.86–2.76 (m, 1H), 2.70–2.60 (m, 1H), 1.25 (d, $J=6.0$ Hz, 6H), 1.13 (d, $J=6.1$ Hz, 3H), 1.08 (d, $J=6.2$ Hz, 3H), 1.03 (t, $J=7.1$ Hz, 3H); ^{13}C NMR ($\text{DMSO}-d_6$): δ 166.9, 157.4, 152.2, 151.1, 150.8, 146.8, 140.4, 138.1, 131.6, 119.5, 118.5, 118.0, 117.2, 109.9, 81.2, 74.4, 70.0, 61.5, 60.2, 56.6, 51.3, 35.1 ($\times 2$), 27.4, 22.3, 22.1, 22.0, 21.9, 15.7. HR-ESMS calcd. for $\text{C}_{29}\text{H}_{39}\text{N}_2\text{O}_8$ $^+$ [M + H] 543.2701, found 543.2711.

(R)-5-((S)-4,5-Dimethoxy-3-oxo-1,3-dihydroisobenzofuran-1-yl)-N-ethyl-4-methoxy-7,8-dihydro[1,3]dioxolo[4,5-g]isoquinoline-2,2-d₂-6(5H)-carboxamide (13e). Compound **13e** was synthesised from **12** (240 mg, 0.522 mmol) according to General Procedure B, with K_2CO_3 (217 mg, 1.57 mmol) and diiodomethane- d_2 (64 μL , 0.784 mmol). The product was obtained as a pale yellow oil (103 mg, 42%). ^1H NMR (CDCl_3): δ 7.06 (d, $J=8.3$ Hz, 1H), 6.70 (d, $J=8.2$ Hz, 1H), 6.33 (s, 1H), 5.94 (dd, $J=3.2$, 0.6 Hz, 1H), 5.68 (d, $J=3.1$ Hz, 1H), 4.94 (br s, 1H), 4.01 (s, 3H), 3.85 (s, 3H), 3.83 (s, 3H), 3.62–3.51 (m, 1H), 3.39–3.18 (m, 2H), 2.82–2.58 (m, 2H), 2.55–2.44 (m, 1H), 1.18 (t, $J=7.2$ Hz, 3H); ^{13}C NMR (CDCl_3): δ 167.3, 158.9, 152.6, 149.0, 148.1, 140.1, 139.8, 134.0, 131.4, 118.8, 118.6, 118.5,

115.1, 102.8, 81.7, 62.5, 59.2, 56.9, 53.7, 39.2, 36.0, 28.2, 15.7. HR-ESMS calcd. for $C_{24}H_{25}D_2N_2O_8^+$ [M + H] 473.1887, found 473.1880.

(R)-6-((S)-4,5-Dimethoxy-3-oxo-1,3-dihydroisobenzofuran-1-yl)-N-ethyl-5-methoxy-2,3,8,9-tetrahydro-[1,4]dioxino[2,3-g]isoquinoline-7(6H)-carboxamide (13f). Compound **13f** was synthesised from **12** (209 mg, 0.456 mmol) according to General Procedure B, with K_2CO_3 (190 mg, 1.38 mmol) and 1,2-dibromoethane (59 μ L, 0.684 mmol). No precipitation was observed following addition to ice. The aqueous layer was extracted with EtOAc (3 \times 10 mL) and solvent removed *in vacuo* to yield the crude product. The product was purified with flash column chromatography (EtOAc) and obtained as a pale yellow foam (131 mg, 60%). 1H NMR (DMSO- d_6): δ 7.37 (d, J = 8.4 Hz, 1H), 6.72 (d, J = 8.3 Hz, 1H), 6.56–6.48 (m, 2H), 5.77 (d, J = 5.4 Hz, 1H), 5.66 (d, J = 5.2 Hz, 1H), 4.31–4.17 (m, 4H), 3.85 (s, 3H), 3.82 (s, 3H), 3.67 (s, 3H), 3.40–3.34 (m, 1H), 3.09–3.00 (m, 2H), 2.91–2.81 (m, 1H), 2.76–2.67 (m, 1H), 2.66–2.56 (m, 1H), 1.00 (t, J = 7.1 Hz, 3H); ^{13}C NMR (DMSO- d_6): δ 167.3, 157.8, 152.7, 147.3, 145.6, 144.1, 141.0, 135.3, 128.7, 120.1, 118.8, 118.5, 118.3, 111.7, 81.0, 64.5, 64.4, 61.9, 60.7, 57.1, 55.4, 51.2, 35.5, 27.1, 16.1. HR-ESMS calcd. for $C_{25}H_{29}N_2O_8^+$ [M + H] 485.1918, found 485.1927.

(R)-7-((S)-4,5-Dimethoxy-3-oxo-1,3-dihydroisobenzofuran-1-yl)-N-ethyl-6-methoxy-3,4,9,10-tetrahydro-2H-[1,4]dioxepino[2,3-g]isoquinoline-8(7H)-carboxamide (13g). Compound **13g** was synthesised from **12** (203 mg, 0.443 mmol) according to General Procedure B, with K_2CO_3 (306 mg, 2.22 mmol) and 1,3-dibromopropane (50 μ L, 0.488 mmol). The product was obtained as a yellow oil (43 mg, 19%). 1H NMR (CDCl $_3$): δ 6.99 (d, J = 8.3 Hz, 1H), 6.53 (s, 1H), 6.41 (d, J = 8.2 Hz, 1H), 6.02 (d, J = 2.7 Hz, 1H), 5.57 (d, J = 2.7 Hz, 1H), 5.04 (s, 1H), 4.31–4.22 (m, 2H), 4.15–4.06 (m, 2H), 4.01 (s, 3H), 3.85 (s, 3H), 3.83 (s, 3H), 3.73–3.63 (m, 1H), 3.36–3.15 (m, 2H), 2.69–2.47 (m, 2H), 2.29–2.10 (m, 3H), 1.17 (t, J = 7.2 Hz, 3H); ^{13}C NMR (CDCl $_3$): δ 167.1, 159.1, 152.7, 152.4, 148.8, 148.2, 143.0, 140.0, 131.4, 118.7, 118.5, 118.3, 118.2, 116.2, 81.0, 71.4, 70.9, 62.5, 61.2, 56.8, 54.0, 38.6, 36.0, 32.0, 27.3, 15.6. HR-ESMS calcd. for $C_{26}H_{31}N_2O_8^+$ [M + H] 499.2075, found 499.2082.

(R)-8-((S)-4,5-Dimethoxy-3-oxo-1,3-dihydroisobenzofuran-1-yl)-N-ethyl-7-methoxy-2,3,4,5,10,11-hexahydro-[1,4]dioxocino[2,3-g]isoquinoline-9(8H)-carboxamide (13h). Compound **13h** was synthesised from **12** (201 mg, 0.438 mmol) according to General Procedure B, with K_2CO_3 (302 mg, 2.19 mmol) and 1,4-dibromobutane (56 μ L, 0.482 mmol). The product was obtained as a white foam (31 mg, 14%). 1H NMR (CDCl $_3$): δ 7.03 (d, J = 8.2 Hz, 1H), 6.54 (s, 1H), 6.41 (d, J = 8.2 Hz, 1H), 6.02 (d, J = 3.4 Hz, 1H), 5.62 (d, J = 3.4 Hz, 1H), 4.96 (s, 1H), 4.44–4.34 (m, 2H), 4.31–4.10 (m, 2H), 4.02 (s, 3H), 3.85 (s, 6H), 3.72–3.61 (m, 1H), 3.54–3.41 (m, 1H), 3.37–3.21 (m, 2H), 2.68–2.61 (m, 2H), 2.12–1.79 (m, 4H), 1.20 (d, J = 7.2 Hz, 3H); ^{13}C NMR (CDCl $_3$): δ 167.1, 159.0, 152.6, 151.5, 149.8, 148.2, 140.5, 140.0, 131.9, 118.8, 118.5, 118.4, 118.1, 116.4, 81.4, 73.1, 72.9, 62.5, 61.1, 56.9, 54.0, 39.0, 36.0, 27.9, 27.5, 26.7, 15.6. HR-ESMS calcd. for $C_{27}H_{33}N_2O_8^+$ [M + H] 513.2231, found 513.2240.

(R)-1-((S)-4,5-Dimethoxy-1,3-dihydroisobenzofuran-1-yl)-N-ethyl-6,7,8-trimethoxy-3,4-dihydroisoquinoline-2(1H)-carboxamide (14a). Compound **14a** was synthesised from **13a** (130 mg, 0.267 mmol) according to General Procedure C, with $NaBH_4$ (30 mg, 0.801 mmol) and $BF_3 \cdot Et_2O$ (428 μ L, 3.47 mmol). The product was obtained as an off-white solid (95 mg, 75%). 1H NMR (CD $_3$ OD): δ 6.78 (d, J = 8.2 Hz, 1H), 6.58 (s, 1H), 6.19 (s, 1H), 5.72 (s, 1H), 5.50 (d, J = 5.6 Hz, 1H), 5.02 (d, J = 12.3 Hz, 1H), 4.92 (d, J = 5.6 Hz, 1H), 3.85 (s, 6H), 3.79 (s, 3H), 3.77 (s, 3H), 3.76 (s, 3H), 3.74–3.70 (m, 1H), 3.64–3.56 (m, 1H), 3.29–3.15 (m, 2H), 2.67–2.57 (m, 2H), 1.16 (t, J = 7.2 Hz, 3H); ^{13}C NMR (CD $_3$ OD): δ 154.3, 153.2, 151.5, 149.2, 142.0, 141.3, 133.6, 133.4, 120.1, 118.9, 118.9, 113.7, 108.4, 87.6, 72.4, 72.3, 61.3,

61.2, 60.5, 56.7, 56.4, 36.7, 36.6, 29.1, 16.0. HR-ESMS calcd. for $C_{25}H_{33}N_2O_7^+$ [M + H] 473.2282, found 473.2294.

(R)-6,7-Bis(difluoromethoxy)-1-((S)-4,5-dimethoxy-1,3-dihydroisobenzofuran-1-yl)-N-ethyl-8-methoxy-3,4-dihydroisoquinoline-2(1H)-carboxamide (14b). Compound **14b** was synthesised from **13b** (130 mg, 0.233 mmol) according to General Procedure C, with $NaBH_4$ (44 mg, 1.17 mmol) and $BF_3 \cdot Et_2O$ (1.12 mL, 9.10 mmol). The product was obtained as a colourless oil (42 mg, 33%). 1H NMR (CDCl $_3$): δ 6.78 (s, 1H), 6.63 (d, J = 8.2 Hz, 1H), 6.75–6.37 (m, 1H), 6.49 (dd, J = 75.4, 73.8 Hz, 1H), 5.96 (d, J = 8.0 Hz, 1H), 5.87–5.80 (m, 2H), 5.36 (d, J = 3.5 Hz, 1H), 5.11 (s, 2H), 3.97 (s, 3H), 3.92–3.84 (m, 1H), 3.81 (s, 3H), 3.80 (s, 3H), 3.40–3.12 (m, 2H), 2.72–2.61 (m, 1H), 2.50–2.35 (m, 1H), 2.28–2.15 (m, 1H), 1.18 (t, J = 7.2 Hz, 3H); ^{19}F NMR (CDCl $_3$): δ –80.98 (d, J = 163.9 Hz), –81.10 (d, J = 163.1 Hz), –81.62 (d, J = 163.8 Hz), –82.04 (d, J = 163.1 Hz); ^{13}C NMR (CDCl $_3$): δ 159.7, 151.9, 150.6, 143.5 (app t, J = 2.8 Hz), 143.4, 136.4, 133.6 (app t, J = 3.2 Hz), 132.1, 131.4, 123.9, 117.1, 116.9 (app t, J = 262.6 Hz), 116.1, 115.8 (app t, J = 262.8 Hz), 112.4, 86.1, 72.0, 61.5, 60.2, 56.5, 56.4, 37.8, 35.8, 28.1, 15.8. HR-ESMS calcd. for $C_{25}H_{29}F_4N_2O_7^+$ [M + H] 545.1905, found 545.1918.

(R)-1-((S)-4,5-Dimethoxy-1,3-dihydroisobenzofuran-1-yl)-N-ethyl-8-methoxy-6,7-bis(methoxy- d_3)-3,4-dihydroisoquinoline-2(1H)-carboxamide (14c). Compound **14c** was synthesised from **13c** (167 mg, 0.338 mmol) according to General Procedure C, with $NaBH_4$ (64 mg, 1.69 mmol) and $BF_3 \cdot Et_2O$ (1.63 mL, 13.2 mmol). The product was obtained as a colourless oil (74 mg, 46%). 1H NMR (CDCl $_3$): δ 6.58 (d, J = 8.2 Hz, 1H), 6.38 (s, 1H), 6.00 (s, 1H), 5.93–5.83 (m, 2H), 5.27 (d, J = 3.5 Hz, 1H), 5.20–5.07 (m, 2H), 3.97 (s, 3H), 3.95–3.87 (m, 1H), 3.81 (s, 3H), 3.78 (s, 3H), 3.40–3.14 (m, 2H), 2.68–2.55 (m, 1H), 2.32–2.18 (m, 1H), 2.12–1.99 (m, 1H), 1.18 (t, J = 7.2 Hz, 3H); ^{13}C NMR (CDCl $_3$): δ 160.0, 152.7, 151.7, 150.1, 143.3, 140.0, 132.2, 132.2, 131.9, 117.4, 117.3, 112.2, 107.2, 86.2, 71.9, 60.9, 60.2, 56.6, 56.3, 37.8, 35.7, 28.2, 15.8. HR-ESMS calcd. for $C_{25}H_{27}D_6N_2O_7^+$ [M + H] 479.2659, found 479.2663.

(R)-1-((S)-4,5-Dimethoxy-1,3-dihydroisobenzofuran-1-yl)-N-ethyl-6,7-diisopropoxy-8-methoxy-3,4-dihydroisoquinoline-2(1H)-carboxamide (14d). Compound **14d** was synthesised from **13d** (588 mg, 1.08 mmol) according to General Procedure C, with $NaBH_4$ (205 mg, 5.42 mmol) and $BF_3 \cdot Et_2O$ (5.22 mL, 42.3 mmol). The product was obtained as a yellow oil (43 mg, 8%). 1H NMR (CDCl $_3$): δ 6.57 (d, J = 8.2 Hz, 1H), 6.39 (s, 1H), 6.01 (s, 1H), 5.94–5.81 (m, 2H), 5.28 (d, J = 3.6 Hz, 1H), 5.22–5.07 (m, 2H), 4.62–4.48 (m, 1H), 4.43–4.32 (m, 1H), 3.98 (s, 3H), 3.96–3.90 (m, 1H), 3.81 (s, 3H), 3.79 (s, 3H), 3.39–3.14 (m, 2H), 2.67–2.54 (m, 1H), 2.29–2.16 (m, 1H), 2.12–1.99 (m, 1H), 1.36 (app t, J = 6.1 Hz, 6H), 1.30 (dd, J = 6.2, 3.0 Hz, 6H), 1.19 (t, J = 7.2 Hz, 3H); ^{13}C NMR (CDCl $_3$): δ 160.2, 151.7, 151.5, 151.2, 143.4, 139.1, 132.2, 132.0, 131.8, 117.4, 117.2, 112.2, 110.4, 86.2, 75.5, 71.9, 70.8, 60.9, 60.2, 56.7, 56.4, 37.9, 35.8, 28.2, 22.6, 22.6, 22.3, 22.1, 15.9. HR-ESMS calcd. for $C_{29}H_{41}N_2O_7^+$ [M + H] 528.2830, found 528.2772.

(R)-5-((S)-4,5-Dimethoxy-1,3-dihydroisobenzofuran-1-yl)-N-ethyl-4-methoxy-7,8-dihydro-[1,3]dioxolo[4,5-g]isoquinoline-2,2- d_2 -6(5H)-carboxamide (14e). Compound **14e** was synthesised from **13e** (94 mg, 0.199 mmol) according to General Procedure C, with $NaBH_4$ (38 mg, 0.994 mmol) and $BF_3 \cdot Et_2O$ (957 μ L, 7.75 mmol). The product was obtained as a colourless oil (14 mg, 16%). 1H NMR (CDCl $_3$): δ 6.62 (d, J = 8.2 Hz, 1H), 6.32 (s, 1H), 6.02 (d, J = 8.1 Hz, 1H), 5.97 (s, 1H), 5.80 (t, J = 3.0 Hz, 1H), 5.32 (d, J = 3.5 Hz, 1H), 5.20–5.07 (m, 2H), 4.04 (s, 3H), 3.87–3.83 (m, 1H), 3.82 (s, 3H), 3.81 (s, 3H), 3.41–3.15 (m, 2H), 2.63–2.51 (m, 1H), 2.31–2.11 (m, 2H), 1.19 (t, J = 7.2 Hz, 3H); ^{13}C NMR (CDCl $_3$): δ 160.0, 151.7, 148.6, 143.3, 139.9, 134.3, 132.2, 131.9, 131.1, 117.7, 116.6, 112.2, 103.0, 86.2, 71.9, 60.3, 59.6, 56.6, 56.4, 38.1, 35.8, 28.3, 15.8. HR-ESMS calcd. for $C_{24}H_{27}D_2N_2O_7^+$ [M + H] 459.2095, found 459.2102.

(*R*)-6-((*S*)-4,5-Dimethoxy-1,3-dihydroisobenzofuran-1-yl)-*N*-ethyl-5-methoxy-2,3,8,9-tetrahydro[1,4]dioxino[2,3-*g*]isoquinoline-7(6*H*)-carboxamide (**14f**). Compound **14f** was synthesised from **13f** (220 mg, 0.453 mmol) according to General Procedure C, with NaBH₄ (223 mg, 5.89 mmol) and BF₃·Et₂O (2.18 mL, 17.7 mmol). The product was obtained as a colourless oil (50 mg, 25%). ¹H NMR (CDCl₃): δ 6.59 (d, *J* = 8.2 Hz, 1H), 6.42 (s, 1H), 6.10 (s, 1H), 5.91 (d, *J* = 8.2 Hz, 1H), 5.87 (t, *J* = 3.2 Hz, 1H), 5.29 (d, *J* = 3.7 Hz, 1H), 5.23–5.08 (m, 2H), 4.40–4.27 (m, 4H), 3.94 (s, 3H), 3.90–3.84 (m, 1H), 3.83 (s, 3H), 3.80 (s, 3H), 3.43–3.15 (m, 2H), 2.64–2.47 (m, 1H), 2.26–2.06 (m, 2H), 1.19 (t, *J* = 7.2 Hz, 3H); ¹³C NMR (CDCl₃): δ 160.3, 151.8, 145.2, 143.9, 143.3, 135.2, 132.2, 131.7, 129.2, 117.7, 117.5, 112.2, 112.1, 86.4, 71.9, 64.5, 64.5, 60.9, 60.3, 56.7, 56.4, 38.3, 35.9, 27.6, 15.9. HR-ESMS calcd. for C₂₅H₃₁N₂O₇⁺ [M + H] 471.2126, found 471.2124.

(*R*)-7-((*S*)-4,5-Dimethoxy-1,3-dihydroisobenzofuran-1-yl)-*N*-ethyl-6-methoxy-3,4,9,10-tetrahydro-2*H*-[1,4]dioxepino[2,3-*g*]isoquinoline-8(7*H*)-carboxamide (**14g**). Compound **14g** was synthesised from **13g** (495 mg, 0.992 mmol) according to General Procedure C, with NaBH₄ (188 mg, 4.96 mmol) and BF₃·Et₂O (4.77 mL, 38.7 mmol). The product was obtained as a pale yellow oil (58 mg, 12%). ¹H NMR (CDCl₃): δ 6.59–6.52 (m, 1H), 6.50 (s, 1H), 6.03 (s, 1H), 5.89–5.82 (m, 2H), 5.26 (d, *J* = 3.7 Hz, 1H), 5.20–5.04 (m, 2H), 4.39–4.25 (m, 2H), 4.16–4.04 (m, 2H), 3.94 (s, 3H), 3.88–3.81 (m, 1H), 3.79 (s, 3H), 3.77 (s, 3H), 3.40–3.12 (m, 2H), 2.59–2.46 (m, 1H), 2.31–2.22 (m, 1H), 2.21–2.11 (m, 2H), 2.10–2.01 (m, 1H), 1.16 (t, *J* = 7.2 Hz, 3H); ¹³C NMR (CDCl₃): δ 160.1, 151.9, 151.6, 148.6, 143.2, 143.0, 132.1, 131.7, 131.3, 119.6, 117.5, 116.1, 112.1, 86.1, 71.8, 71.4, 70.9, 61.2, 60.1, 56.7, 56.2, 37.8, 35.7, 32.1, 27.5, 15.8. HR-ESMS calcd. for C₂₆H₃₃N₂O₇⁺ [M + H] 485.2282, found 485.2293.

(*R*)-8-((*S*)-4,5-Dimethoxy-1,3-dihydroisobenzofuran-1-yl)-*N*-ethyl-7-methoxy-2,3,4,5,10,11-hexahydro[1,4]dioxino[2,3-*g*]isoquinoline-9(8*H*)-carboxamide (**14h**). Compound **14h** was synthesised from **13h** (251 mg, 0.489 mmol) according to General Procedure C, with NaBH₄ (93 mg, 2.44 mmol) and BF₃·Et₂O (2.35 mL, 19.1 mmol). The product was obtained as a pale yellow oil (14 mg, 6%). ¹H NMR (CDCl₃): δ 6.59 (d, *J* = 8.2 Hz, 1H), 6.51 (s, 1H), 6.01 (br s, 1H), 5.92–5.83 (m, 2H), 5.30 (d, *J* = 3.7 Hz, 1H), 5.22–5.08 (m, 2H), 4.43–4.22 (m, 4H), 3.98 (s, 3H), 3.92–3.84 (m, 1H), 3.82 (s, 3H), 3.79 (s, 3H), 3.43–3.14 (m, 2H), 2.66–2.47 (m, 1H), 2.28–2.16 (m, 1H), 2.15–2.02 (m, 1H), 1.97–1.86 (m, 4H), 1.18 (t, *J* = 7.2 Hz, 3H); ¹³C NMR (CDCl₃): δ 160.1, 151.7, 150.9, 149.7, 143.3, 140.8, 132.2, 131.9, 131.8, 119.5, 117.5, 116.6, 112.2, 86.3, 73.0, 71.9, 61.2, 60.2, 56.8, 56.3, 38.0, 35.8 (×2), 27.9, 27.7, 27.0, 15.9. HR-ESMS calcd. for C₂₇H₃₅N₂O₇⁺ [M + H] 499.2439, found 499.2444.

(*S*)-6,7-Dimethoxy-3-((*R*)-4-methoxy-6-((1-methyl-1*H*-imidazol-4-yl)sulfonyl)-5,6,7,8-tetrahydro[1,3]dioxolo[4,5-*g*]isoquinolin-5-yl)isobenzofuran-1(3*H*)-one (**15**). To a solution of **10** (299 mg, 0.749 mmol) dissolved in DCM (2 mL) was added Et₃N (313 μL, 2.25 mmol) and the mixture was left to stir at 25 °C for 15 min. 1-Methyl-1*H*-imidazole-4-sulfonyl chloride (154 mg, 0.786 mmol) was then added and the reaction was stirred at 25 °C for 16 h. Following the addition of H₂O (5 mL) to the reaction, the mixture was extracted with DCM (3 × 20 mL) and the organic layer was dried over MgSO₄, filtered and the solvent was removed *in vacuo*. The crude product was purified by flash column chromatography (EtOAc) to yield the title product as a white foam (342 mg, 82%). ¹H NMR (CDCl₃): δ 7.60–7.56 (m, 2H), 7.05 (d, *J* = 8.3 Hz, 1H), 6.42 (dd, *J* = 8.3, 0.5 Hz, 1H), 6.33 (s, 1H), 5.93 (s, 2H), 5.78 (dd, *J* = 4.5, 0.7 Hz, 1H), 5.63 (d, *J* = 4.5 Hz, 1H), 4.02 (s, 3H), 3.94 (s, 3H), 3.86 (s, 3H), 3.76 (s, 3H), 3.60–3.51 (m, 1H), 2.83–2.70 (m, 1H), 2.61–2.47 (m, 2H); ¹³C NMR (CDCl₃): δ 167.3, 152.9, 149.5, 148.4, 142.8, 139.8, 139.6, 137.4, 134.2, 129.6, 127.3, 118.9, 118.6, 118.2, 114.4, 103.2, 101.2, 79.4, 62.5, 59.6, 56.9, 53.2, 40.2, 33.4, 27.4. HR-ESMS calcd. for C₂₅H₂₆N₃O₉S⁺ [M + H] 544.1384, found 544.1399.

(*S*)-3-((*R*)-6,7-Dihydroxy-8-methoxy-2-((1-methyl-1*H*-imidazol-4-yl)sulfonyl)-1,2,3,4-tetrahydroisoquinolin-1-yl)-6,7-dimethoxyisobenzofuran-1(3*H*)-one (**16**). Compound **16** was synthesised from **15** (771 mg, 1.42 mmol) according to General Procedure A, with BCl₃ (1 M in DCM, 2.84 mL, 2.84 mmol). The product was obtained as a pale brown foam (614 mg, 82%). ¹H NMR (CDCl₃): δ 7.41 (d, *J* = 1.0 Hz, 1H), 7.38–7.34 (m, 1H), 7.02 (d, *J* = 8.4 Hz, 1H), 6.48 (d, *J* = 8.3 Hz, 1H), 6.34 (s, 1H), 5.80 (d, *J* = 4.3 Hz, 1H), 5.68 (d, *J* = 4.5 Hz, 1H), 3.95 (s, 3H), 3.81 (s, 3H), 3.76 (s, 3H), 3.68 (s, 3H), 3.55 (dd, *J* = 6.7, 3.9 Hz, 1H), 2.63–2.50 (m, 2H), 2.48–2.36 (m, 1H); ¹³C NMR (CDCl₃): δ 167.9, 152.7, 147.9, 145.8, 144.6, 139.7, 139.4, 139.2, 135.7, 126.7, 124.5, 123.8, 118.9, 118.8, 118.6, 114.7, 110.9, 80.6, 62.4, 60.5, 56.8, 42.7, 40.9, 34.2. HR-ESMS calcd. for C₂₄H₂₆N₃O₉S⁺ [M + H] 532.1384, found 532.1394.

(*S*)-6,7-Dimethoxy-3-((*R*)-5-methoxy-7-((1-methyl-1*H*-imidazol-4-yl)sulfonyl)-2,3,6,7,8,9-hexahydro[1,4]dioxino[2,3-*g*]isoquinolin-6-yl)isobenzofuran-1(3*H*)-one (**17**). Compound **17** was synthesised from **16** (220 mg, 0.413 mmol) according to General Procedure B, with K₂CO₃ (171 mg, 1.24 mmol) and 1,2-dibromoethane (54 μL, 0.619 mmol). The product was obtained as a clear oil (45 mg, 20%). ¹H NMR (CDCl₃): δ 7.47 (s, 1H), 7.36 (s, 1H), 7.01 (d, *J* = 8.3 Hz, 1H), 6.48 (d, *J* = 8.2 Hz, 1H), 6.41 (s, 1H), 5.88 (d, *J* = 4.2 Hz, 1H), 5.80 (d, *J* = 4.2 Hz, 1H), 4.26 (s, 4H), 3.98 (s, 3H), 3.84 (s, 6H), 3.75 (s, 3H), 3.71–3.64 (m, 1H), 2.88–2.71 (m, 1H), 2.68–2.49 (m, 2H); ¹³C NMR (CDCl₃): δ 167.3, 152.7, 148.1, 145.4, 144.3, 140.3, 139.8, 138.7, 135.3, 128.2, 124.0, 118.8, 118.6, 118.5, 116.2, 112.3, 80.8, 64.4, 64.4, 62.5, 61.0, 56.8, 53.4, 41.1, 34.1, 27.4. HR-ESMS calcd. for C₂₆H₂₈N₃O₉S⁺ [M + H] 558.1541, found 558.1543.

(*R*)-10-Chloro-6-((*S*)-4,5-dimethoxy-3-oxo-1,3-dihydroisobenzofuran-1-yl)-*N*-ethyl-5-methoxy-2,3,8,9-tetrahydro[1,4]dioxino[2,3-*g*]isoquinoline-7(6*H*)-carboxamide (**18**). To a cooled (–5 °C) solution of **13f** (174 mg, 0.359 mmol) in CHCl₃ (9 mL) was added a solution of SO₂Cl₂ (87 μL, 1.08 mmol) diluted in CHCl₃ (9 mL) dropwise. The reaction was warmed to 25 °C and stirred for 2 h. The reaction was then pipetted over ice (~20 g) and neutralised with sat. aq. NaHCO₃. The mixture was extracted with CHCl₃ (3 × 50 mL), with the organic layer dried over anhydrous MgSO₄, filtered and concentrated *in vacuo* to yield the crude product as a pale yellow foam. The crude product was then purified by flash column chromatography (EtOAc) to give the title product as a white foam (140 mg, 75%). ¹H NMR (CDCl₃): δ 6.99 (d, *J* = 8.3 Hz, 1H), 6.47 (d, *J* = 8.3 Hz, 1H), 5.92 (d, *J* = 3.5 Hz, 1H), 5.58 (d, *J* = 3.6 Hz, 1H), 5.08 (s, 1H), 4.39–4.29 (m, 2H), 4.29–4.20 (m, 2H), 3.96 (s, 3H), 3.79 (s, 3H), 3.77 (s, 3H), 3.72–3.63 (m, 1H), 3.31–3.09 (m, 2H), 2.68–2.56 (m, 2H), 2.26–2.12 (m, 1H), 1.10 (t, *J* = 7.2 Hz, 3H); ¹³C NMR (CDCl₃): δ 167.1, 159.0, 152.8, 148.5, 143.9, 140.7, 139.7, 135.9, 127.2, 118.9, 118.6, 118.1, 117.2, 116.5, 80.9, 65.0, 64.1, 62.6, 61.0, 56.9, 53.6, 38.2, 36.1, 24.8, 15.7. HR-ESMS calcd. for C₂₅H₂₈ClN₂O₈⁺ [M + H] 519.1529, found 519.1540.

(*S*)-3-((*R*)-10-Chloro-5-methoxy-7-((1-methyl-1*H*-imidazol-4-yl)sulfonyl)-2,3,6,7,8,9-hexahydro[1,4]dioxino[2,3-*g*]isoquinolin-6-yl)-6,7-dimethoxyisobenzofuran-1(3*H*)-one (**19**). To a cooled (–5 °C) solution of **17** (120 mg, 0.215 mmol) in CHCl₃ (5 mL) was added a solution of SO₂Cl₂ (52 μL, 0.646 mmol) diluted in CHCl₃ (5 mL) dropwise. The reaction was warmed to 25 °C and stirred for 2 h. The reaction was then pipetted over ice (~20 g) and neutralised with sat. aq. NaHCO₃. The mixture was extracted with CHCl₃ (3 × 50 mL), with the organic layer dried over anhydrous MgSO₄, filtered and concentrated *in vacuo* to yield the crude product as a pale yellow foam. The crude product was then purified by flash column chromatography (EtOAc) to give the title product as a white foam (40 mg, 31%). ¹H NMR (CDCl₃): δ 7.45 (d, *J* = 1.2 Hz, 1H), 7.33 (d, *J* = 0.8 Hz, 1H), 7.03 (d, *J* = 8.3 Hz, 1H), 6.54 (d, *J* = 8.3 Hz, 1H), 5.83 (d, *J* = 4.2 Hz, 1H), 5.78 (d, *J* = 4.2 Hz, 1H), 4.41–4.34 (m, 2H), 4.33–4.24 (m, 2H), 3.99 (s, 3H), 3.84 (s, 3H), 3.82 (s, 3H),

3.81–3.75 (m, 1H), 3.73 (s, 3H), 2.85–2.72 (m, 1H), 2.68–2.54 (m, 2H); ^{13}C NMR (CDCl_3): δ 167.2, 152.8, 148.2, 143.9, 140.7, 140.1, 139.7, 138.8, 135.9, 126.0, 124.0, 118.8, 118.6, 118.2, 117.1, 116.4, 80.3, 64.9, 64.1, 62.5, 61.0, 56.8, 53.2, 40.2, 34.1, 24.8. HR-ESMS calcd. for $\text{C}_{26}\text{H}_{27}\text{ClN}_3\text{O}_5\text{S}^+$ $[\text{M} + \text{H}]$ 592.1151, found 592.1165.

(R)-10-Chloro-6-((S)-4,5-dimethoxy-1,3-dihydroisobenzofuran-1-yl)-N-ethyl-5-methoxy-2,3,8,9-tetrahydro[1,4]dioxino[2,3-g]isoquinoline-7(6H)-carboxamide (20). Compound 20 was synthesised from 18 (139 mg, 0.267 mmol) according to General Procedure C, with NaBH_4 (30 mg, 0.801 mmol) and $\text{BF}_3 \cdot \text{Et}_2\text{O}$ (428 μL , 3.47 mmol). The product was obtained as a white foam (64 mg, 47%). ^1H NMR (CDCl_3): δ 6.59 (d, $J = 8.2$ Hz, 1H), 5.93 (d, $J = 8.2$ Hz, 1H), 5.85 (m, 1H), 5.27 (d, $J = 3.7$ Hz, 1H), 5.15 (m, 2H), 4.42–4.37 (m, 2H), 4.37–4.28 (m, 2H), 3.98–3.93 (m, 1H), 3.92 (s, 3H), 3.81 (s, 3H), 3.78 (s, 3H), 3.38–3.26 (m, 1H), 3.25–3.12 (m, 1H), 2.59–2.47 (m, 1H), 2.45–2.35 (m, 1H), 2.10–1.97 (m, 1H), 1.17 (t, $J = 7.2$ Hz, 3H); ^{13}C NMR (CDCl_3): δ 159.8, 151.7, 143.7, 143.3, 140.2, 135.8, 132.0, 131.5, 127.1, 118.3, 117.3, 116.3, 112.2, 86.1, 71.9, 64.9, 64.1, 61.0, 60.2, 56.3, 56.2, 37.3, 35.7, 25.1, 15.8. HR-ESMS calcd. for $\text{C}_{25}\text{H}_{30}\text{ClN}_2\text{O}_7^+$ $[\text{M} + \text{H}]$ 505.1736, found 505.1745.

(R)-10-Chloro-6-((S)-4,5-dimethoxy-1,3-dihydroisobenzofuran-1-yl)-5-methoxy-7-((1-methyl-1H-imidazol-4-yl)sulfonyl)-2,3,6,7,8,9-hexahydro[1,4]dioxino[2,3-g]isoquinoline (21). Compound 21 was synthesised from 19 (120 mg, 0.202 mmol) according to General Procedure C, with NaBH_4 (38 mg, 1.01 mmol) and $\text{BF}_3 \cdot \text{Et}_2\text{O}$ (973 μL , 7.89 mmol). The product was obtained as a yellow oil (61 mg, 52%). ^1H NMR (CDCl_3): δ 7.33 (s, 2H), 6.67 (d, $J = 8.2$ Hz, 1H), 6.28 (d, $J = 8.2$ Hz, 1H), 5.59 (d, $J = 2.4$ Hz, 1H), 5.47 (d, $J = 4.5$ Hz, 1H), 5.11 (dd, $J = 12.4$, 2.4 Hz, 1H), 5.03 (d, $J = 12.3$ Hz, 1H), 4.40–4.33 (m, 2H), 4.33–4.22 (m, 2H), 3.80 (s, 6H), 3.77 (s, 4H), 3.64 (s, 3H), 2.85–2.71 (m, 1H), 2.69–2.57 (m, 1H), 2.55–2.43 (m, 1H); ^{13}C NMR (CDCl_3): δ 151.6, 144.0, 143.1, 140.3, 140.0, 138.8, 135.7, 132.6, 132.3, 125.7, 123.9, 118.7, 117.5, 115.9, 112.1, 85.0, 71.9, 64.9, 64.1, 60.8, 60.0, 56.3, 55.4, 39.9, 34.0, 24.1. HR-ESMS calcd. for $\text{C}_{26}\text{H}_{29}\text{ClN}_3\text{O}_8\text{S}^+$ $[\text{M} + \text{H}]$ 578.1358, found 578.1371.

Biology

Compound preparation and storage: A 10^{-2} M stock solution was prepared for each compound by dissolving the compound in sterile-filtered DMSO (Sigma D2650), and the solution was stored at -20°C until use.

Cell culture and reagents: Human breast cancer cell line MCF-7 (HTB-22) and pancreatic cancer cell line PANC-1 (CRL-1469) were purchased directly from American Type Culture Collection (ATCC) and cultured in minimum essential medium alpha (MEM α) (Invitrogen 32561-037) and Dulbecco's modified eagle medium (DMEM) (Invitrogen 10566-016) supplemented with 10% foetal bovine serum (FBS) (Invitrogen 10100-147), respectively. MDR cell line NCI/Ad $^{\text{RES}}$ was a gift from Prof. Kenneth H. Cowan at the National Cancer Institute.^[40] Cells were cultured in a humidified atmosphere containing 5% CO_2 at 37°C . Before use, cell lines were tested for the presence of mycoplasma by using a MycoAlert Mycoplasma detection kit as per manufacturer's instructions; cells employed in the assays tested negative for mycoplasma.

Cell viability assays: MCF-7 and PANC-1 cells were seeded at 5×10^3 cells per well in 96-well plates 16 h before treatment. Cells were then treated with various concentrations of noscapine analogues. After 72 h of treatment, cell viability was determined following incubation with resazurin dye (CellTiter-Blue assay–Promega G8080). The emitted fluorescence was detected using Envision microplate reader (PerkinElmer) at 560 nm excitation/590 nm emission wavelengths. The obtained fluorescence values were

plotted against log concentration of the inhibitor, and EC_{50} values were calculated using GraphPad Prism statistical software (v7).

Cell cytotoxicity assays: MCF-7 and NCI/Ad $^{\text{RES}}$ cells were both cultured in high-glucose (25 mM) DMEM supplemented with 10% FBS and 100 U/mL penicillin and 100 $\mu\text{g}/\text{mL}$ streptomycin. Every third passage, the NCI/Ad $^{\text{RES}}$ cells were treated with 3 μM doxorubicin to maintain selection pressure for the resistance phenotype. Cells were seeded at a density of 3×10^3 cells per well in 96-well plates and recovered in standard culture condition for 48 hours prior to drug treatment. Following the addition of compounds, cells were incubated for a further 96 h before measuring the number of live cells using a standard MTT assay.

The percentage of live cells was plotted as a function of drug concentration and fitted with the general dose response relationship. The extent of cell death and the drug potency EC_{50} were estimated from the non-linear regression using GraphPad Prism (v5). The EC_{50} values of noscapine and the derivatives were compared using One-way ANOVA with the Bonferroni post-hoc test. A value of $p < 0.05$ was considered statistically significant.

Tubulin polymerisation assay: Tubulin polymerisation was recorded turbidimetrically at 340 nm in PerkinElmer EnVision2101 Multilabel Reader equipped with temperature controllers. Compounds of interest (2 mM in sterile-filtered DMSO) were dissolved in General Tubulin Buffer (80 mM PIPES pH 6.9, 2 mM MgCl_2 , 0.5 mM EGTA) to a final concentration of 10 μM and were added to 96-half area well plate and kept at 37°C . Tubulin was dissolved to a final concentration of 3 mg/mL in 80 mM PIPES pH 6.9, 0.5 mM MgCl_2 , 0.5 mM EGTA, 1 mM GTP, 10.2% glycerol and was kept at 4°C prior to addition to plate. Kinetic absorbance reading started immediately following addition of tubulin to the plate, and was recorded at 37°C over a period of 60 min. The tubulin polymerisation assay kit (BK006P) used to conduct this study was supplied by Cytoskeleton Inc.

Structural studies

Crystallisation, data collection and structure determination: $\text{T}_2\text{R-TTL}$ crystals were grown as previously described by Prota *et al.*^[38,39] via the vapor diffusion method. Crystals grew over more than 2 days in reservoir solution containing 4% PEG 4 K, 7% glycerol, 30 mM MgCl_2 , 30 mM CaCl_2 , 5 mM tyrosine and 100 mM MES/Imidazole pH 6.5. Compound 14e was soaked into crystals overnight at 20°C at a final concentration of 5 mM in reservoir solution. Subsequently, the crystals were transferred into two cryoprotectant solutions (i) 10% PEG 4 K, 16% glycerol, 30 mM MgCl_2 , 30 mM CaCl_2 , 5 mM tyrosine, 100 mM MES/Imidazole pH 6.5 and (ii) 10% PEG 4 K, 22% glycerol, 30 mM MgCl_2 , 30 mM CaCl_2 , 5 mM tyrosine, 100 mM MES/Imidazole pH 6.5 and then flash-cooled in liquid nitrogen. X-Ray diffraction data were collected at 100 K at the beamline X06DA of the Swiss Light Source (Paul Scherrer Institut, Villigen PSI, Switzerland). The obtained data were processed and merged using XDS^[41] to 2.2 Å resolution. The $\text{T}_2\text{R-TTL-14e}$ structure was determined in Phenix^[42] by the difference Fourier method using a $\text{T}_2\text{R-TTL}$ complex template model in the absence of ligands and solvent molecules (PDB ID 5LXT). Difference density delineating the shape of a compound was observed after three cycles of rigid body and restrained refinement using Phenix.^[42] After correction of geometry, Ramachandran and rotamer outliers and the addition of solvent molecules, compound 14e was inserted into the density. Refmac^[43] was used to concomitantly refine the β -T7 loop and compound 14e in order to estimate the occupancy level of the ligand. The quality of the $\text{T}_2\text{R-TTL-14e}$ structure was assessed using MolProbity.^[44] The final model was refined to 2.20 Å resolution with crystallographic R values of 17.8% (R_{work}) and 21.3% (R_{free}). Small

root-mean-square deviations (rmsd) from ideal values for bond lengths and bond angles show the good geometry of the refined model. PyMOL (the PyMOL Molecular Graphics System, Version 2.3.2, Schrödinger, LLC) was used to generate the molecular graphics.

PDB ID Codes

Coordinates and structure factors of the T₂R-TTL-14e complex have been deposited at the Protein Data Bank (www.rcsb.org) under accession number PDB: 7AU5. Authors will release the atomic coordinates and experimental data upon article publication.

Acknowledgements

The authors would like to thank the Australian government for their support through an Australian Postgraduate Award to CY. The authors also thank the National Cancer Institute (NCI) for screening selected compounds in their NCI-60 Human Tumour Cell Lines Screen, and the staff of the Swiss Light Source responsible for beamline X06DA, for their support during X-ray data collection. This work was supported by the H2020-MSCA-ITN-2019 (860070 TUBINTRAIN; to AEP) and the Swiss National Science Foundation (310030_192566; to MOS).

Conflict of Interest

The authors declare no conflict of interest.

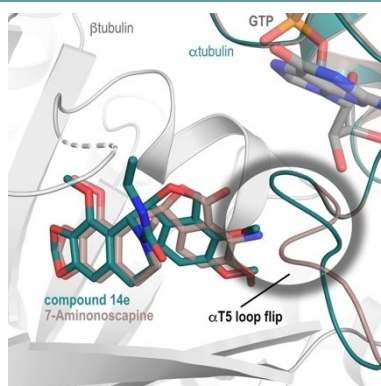
Keywords: noscapine derivatives • anti-cancer agents • microtubule targeting agents • anti-mitotic agents

- [1] E. Pasquier, M. Kavallaris, *IUBMB Life* **2008**, *60*, 165–170.
- [2] G. M. Cragg, J. M. Pezzuto, *Med. Princ. Pract.* **2016**, *25*, 41–59.
- [3] A. Rayan, J. Raiyn, M. Falah, *PLoS One* **2017**, *12*, e0187925.
- [4] A. DeBono, B. Capuano, P. J. Scammells, *J. Med. Chem.* **2015**, *58*, 5699–5727.
- [5] M. Kavallaris, *Nat. Rev. Cancer* **2010**, *10*, 194–204.
- [6] K. Ye, Y. Ke, N. Keshava, J. Shanks, J. A. Kapp, R. R. Tekmal, J. Petros, H. C. Joshi, *Proc. Natl. Acad. Sci. USA* **1998**, *95*, 1601–1606.
- [7] M. Mahmoudian, P. Rahimi-Moghaddam, *Recent Pat. Anti-Cancer Drug Discovery* **2009**, *4*, 92–97.
- [8] B. Dahlström, T. Mellstrand, C.-G. Löfdahl, M. Johansson, *Eur. J. Clin. Pharmacol.* **1982**, *22*, 535–539.
- [9] M. O. Karlsson, B. Dahlström, S.-Å. Eckernäs, M. Johansson, A. Tufvesson Alm, *Eur. J. Clin. Pharmacol.* **1990**, *39*, 275–279.
- [10] A. J. DeBono, S. J. Mistry, J. Xie, D. Muthiah, J. Phillips, S. Ventura, R. Callaghan, C. W. Pouton, B. Capuano, P. J. Scammells, *ChemMedChem* **2014**, *9*, 399–410.
- [11] S. M. Devine, C. Yong, D. Amenuvege, L. Aurelio, D. Muthiah, C. W. Pouton, R. Callaghan, B. Capuano, P. J. Scammells, *J. Med. Chem.* **2018**, *61*, 8444–8456.
- [12] C. Yong, S. M. Devine, X. Gao, A. Yan, R. Callaghan, B. Capuano, P. J. Scammells, *ChemMedChem* **2019**, *14*, 1968–1981.
- [13] D. Muthiah, G. K. Henshaw, A. J. DeBono, B. Capuano, P. J. Scammells, R. Callaghan, *Drug Metab. Dispos.* **2019**, *47*, 164–172.
- [14] J. Zhou, K. Gupta, S. Aggarwal, R. Aneja, R. Chandra, D. Panda, H. C. Joshi, *Mol. Pharmacol.* **2003**, *63*, 799–807.
- [15] R. Aneja, S. N. Vangapandu, M. Lopus, V. G. Visweswarappa, N. Dhiman, A. Verma, R. Chandra, D. Panda, H. C. Joshi, *Biochem. Pharmacol.* **2006**, *72*, 415–426.
- [16] R. Aneja, S. N. Vangapandu, M. Lopus, R. Chandra, D. Panda, H. C. Joshi, *Mol. Pharmacol.* **2006**, *69*, 1801–1809.
- [17] P. K. Naik, B. P. Chatterji, S. N. Vangapandu, R. Aneja, R. Chandra, S. Kantevari, H. C. Joshi, *J. Comput.-Aided Mol. Des.* **2011**, *25*, 443–454.
- [18] S. Santoshi, P. K. Naik, H. C. Joshi, *J. Biomol. Screening* **2011**, *16*, 1047–1058.
- [19] T. Mahaddalkar, P. K. Naik, S. Choudhary, N. Manchukonda, S. Kantevari, M. Lopus, *J. Biomol. Struct. Dyn.* **2016**, *35*, 2475–2484.
- [20] J. T. Anderson, A. E. Ting, S. Boozer, K. R. Brunden, C. Crumrine, J. Danzig, T. Dent, L. Faga, J. J. Harrington, W. F. Hodnick, S. M. Murphy, G. Pawlowski, R. Perry, A. Raber, S. E. Rundlett, A. Stricker-Krongrad, J. Wang, Y. L. Bennani, *J. Med. Chem.* **2005**, *48*, 7096–7098.
- [21] R. C. Mishra, P. Karna, S. R. Gundala, V. Pannu, R. A. Stanton, K. K. Gupta, M. H. Robinson, M. Lopus, L. Wilson, M. Henary, R. Aneja, *Biochem. Pharmacol.* **2011**, *82*, 110–121.
- [22] K. B. Mishra, R. C. Mishra, V. K. Tiwari, *RSC Adv.* **2015**, *5*, 51779–51789.
- [23] K. B. Mishra, R. C. Tiwari, P. Bose, R. Singh, A. K. Rawat, S. K. Singh, R. C. Mishra, R. K. Singh, V. K. Tiwari, *ChemistrySelect* **2019**, *4*, 2644–2648.
- [24] Y. L. Bennani, W. Gu, A. Canales, F. J. Diaz, B. K. Eustace, R. R. Hoover, J. Jimenez-Barbero, A. Nezami, T. Wang, *J. Med. Chem.* **2012**, *55*, 1920–1925.
- [25] M. A. Oliva, A. E. Prota, J. Rodríguez-Salarichs, Y. L. Bennani, J. Jiménez-Barbero, K. Bargsten, Á. Canales, M. O. Steinmetz, J. F. Díaz, *J. Med. Chem.* **2020**, *63*, 8495–8501.
- [26] A. J. DeBono, J. H. Xie, S. Ventura, C. W. Pouton, B. Capuano, P. J. Scammells, *ChemMedChem* **2012**, *7*, 2122–2133.
- [27] Y. Kumagai, J. M. Fukuto, A. K. Cho, *Curr. Med. Chem.* **1994**, *1*, 254–261.
- [28] R. Nabbout, C. Chiron, *Eur. J. Paediatr. Neurol.* **2012**, *16*, S13–S17.
- [29] B. D. Schalet, T. Z. Tang, R. J. DeRubeis, S. D. Hollon, J. D. Amsterdam, R. C. Shelton, *PLoS One* **2016**, *11*, e0159647.
- [30] M. Correia, P. Hollenberg, *Cytochrome P450 Structure, Mechanism, and Biochemistry*, Springer, Cham, **2015**, p 177–259.
- [31] D. Mansuy, J. P. Battioni, J. C. Chottard, V. Ullrich, *J. Am. Chem. Soc.* **1979**, *101*, 3971–3973.
- [32] A. R. Dahl, E. Hodgson, *Chem.-Biol. Interact.* **1979**, *27*, 163–175.
- [33] L. Bertilsson, M. L. Dahl, P. Dalén, A. Al-Shurbaji, *Br. J. Clin. Pharmacol.* **2002**, *53*, 111–122.
- [34] K. McCamley, J. A. Ripper, R. D. Singer, P. J. Scammells, *J. Org. Chem.* **2003**, *68*, 9847–9850.
- [35] G. B. Kok, P. J. Scammells, *Org. Biomol. Chem.* **2011**, *9*, 1008–1011.
- [36] R. Krishna, L. D. Mayer, *Eur. J. Pharm. Sci.* **2000**, *11*, 265–283.
- [37] P. E. Ghaly, R. M. Abou El-Magd, C. D. Churchill, J. A. Tuszyński, F. G. West, *Oncotarget* **2016**, *7*, 40518–40530.
- [38] A. E. Prota, K. Bargsten, D. Zurwerra, J. J. Field, J. F. Díaz, K.-H. Altmann, M. O. Steinmetz, *Science* **2013**, *339*, 587–590.
- [39] A. E. Prota, M. M. Magiera, M. Kuijpers, K. Bargsten, D. Frey, M. Wieser, R. Jaussi, C. C. Hoogenraad, R. A. Kammerer, C. Janke, M. O. Steinmetz, *J. Cell Biol.* **2013**, *200*, 259–270.
- [40] G. Batist, A. Tulpule, B. K. Sinha, A. G. Katki, C. E. Myers, K. H. Cowan, *J. Biol. Chem.* **1986**, *261*, 15544–15549.
- [41] W. Kabsch, *Acta Crystallogr. Sect. D* **2010**, *66*, 125–132.
- [42] P. D. Adams, P. V. Afonine, G. Bunkóczi, V. B. Chen, I. W. Davis, N. Echols, J. J. Headd, L. W. Hung, G. J. Kapral, R. W. Grosse-Kunstleve, A. J. McCoy, N. W. Moriarty, R. Oeffner, R. J. Read, D. C. Richardson, J. S. Richardson, T. C. Terwilliger, P. H. Zwart, *Acta Crystallogr. Sect. D* **2010**, *66*, 213–221.
- [43] G. N. Murshudov, P. Skubak, A. A. Lebedev, N. S. Pannu, R. A. Steiner, R. A. Nicholls, M. D. Winn, F. Long, A. A. Vagin, *Acta Crystallogr. Sect. D* **2011**, *67*, 355–367.
- [44] I. W. Davis, L. W. Murray, J. S. Richardson, D. C. Richardson, *Nucleic Acids Res.* **2004**, *32*, W615–619.

Manuscript received: May 24, 2021
Accepted manuscript online: June 22, 2021
Version of record online: ■■■, ■■■■

FULL PAPERS

Key interactions: We describe the design, synthesis and pharmacological evaluation of noscapine derivatives with modifications to the 1,3-benzodioxole moiety. These efforts afforded the deuterated noscapinoid **14e** and the dioxino-containing analogue **20** as potent cytotoxic agents with EC_{50} values of $< 2 \mu\text{M}$ against breast cancer (MCF-7) cells. These compounds were shown to inhibit tubulin polymerisation and were not vulnerable to the overexpression of resistance conferring P-gp efflux pumps in drug-resistant MCF-7 cells. We also conducted X-ray crystallography studies that yielded a high-resolution structure of **14e** bound to tubulin.



Dr. C. Yong, Dr. S. M. Devine, A.-C. Abel, Dr. S. D. Tomlins, Dr. D. Muthiah, X. Gao, Prof. R. Callaghan, Prof. M. O. Steinmetz, Dr. A. E. Prota, Prof. B. Capuano*, Prof. P. J. Scammells**

1 – 14

1,3-Benzodioxole-Modified Noscapine Analogues: Synthesis, Antiproliferative Activity, and Tubulin-Bound Structure

